
We would like to thank the reviewers for their useful comments and suggestions which have helped us to improve the manuscript.

Reviewers' comments

[Reviewer 1](#), [Reviewer 2](#)

**Authors' response is shown in black and bulleted.
Quotes from the manuscript are in italics.**

Please note: Some figure numbers have been changed in the updated version of the manuscript. New figure numbers are referenced in any related comments. Quoted line numbers are from the revised manuscript.

This study presents a very nice series of simulations to test the response of Arctic mixed-phase clouds to subsidence under several different scenarios. This is a very little studied topic for these clouds, and the topic is appropriate for ACP. The authors do a good job of presenting not just the results, but in providing in depth discussion for why the changes occur. However, I have questions about some of their process arguments, and the paper overall needs to be edited substantially for clarity and be made more concise. I recommend major revisions.

Major Comments:

1. This is an extremely long paper, by my estimate 10-11 thousand words. I appreciate that there are several sets of simulations to discuss, but I still found that the paper was very repetitive at times and the writing was not always clear or well organized. I think that it could be substantially shortened without removing any of the main points. I've pointed out several specific instances where improvements could be made below.

- We have scaled back the manuscript by about 3 pages (approximately 2200 words) following Reviewer 1's point. Additionally, we have endeavoured to remove as much repetition as we can to clarify the main points being made. Instead of re-iterating the findings of each test in the subsequent one, we have focused more on what is new in that chosen scenario. We have also ensured that no comparisons between test cases are made in the Results section; these have now been moved to the Discussion.

2. Page 13, Line 8. It seems that the authors have misread the plot. Altering Nice has a much larger impact than changing W_{sub} , not the other way around. This false interpretation is repeated in the conclusions on Page 27, Line 14. This is also an important point for understanding my next comment.

- This is correct, and was also highlighted by Reviewer 2. We did inaccurately describe the plot and have rectified this in the manuscript (now page 12, line

1). This paragraph now begins with: “Trios can be easily identified in Fig. 6(a)...”. We apologise for any confusion caused.

3. The primary hypothesis is that increased subsidence retards dry air entrainment, leading to higher LWP and increased rain formation. The former allows for greater cloud top radiative cooling while the latter allows for greater sub-cloud evaporation and turbulence production. My question though is why do you not see a similar response when decreasing N_{ice} ? When decreasing N_{ice} , you have much higher LWP, more rain production and sub-cloud evaporation, but you do not seem to get much change to TKE. Some differences exist, but they are not nearly as large as the differences due to varying W_{sub} , even though the change in LWP is larger when varying N_{ice} . Why do we not see a similar response?

- This effect can be explained by considering the $\delta Q_{sg}/\delta t$ values in each of these cases. As such, a figure showing $\delta Q_{sg}/\delta t$ and $\delta Q_{rain}/\delta t$ has been added as Fig. 8 to show the differences in tendencies between CNTRL_D10, CNTRL_D10x0.5, and CNTRL_D10x2. The following discussion has been added to the manuscript at page 14, lines 5-15:

“LWP and below-cloud rain evaporation are enhanced in CNTRL_D10x0.5 with comparison to CNTRL_D10 and CNTRL_D10x2; however, w'^2 is not strongly affected (Fig. 6). Figure 8 shows $\delta Q_{sg}/\delta t$ and $\delta Q_{rain}/\delta t$ at 9 h to illustrate differences between the D10x0.5, D10, and D10x2 CNTRL cases. $\delta Q_{sg}/\delta t$ is similar in the D10 and D10x0.5 simulations, whilst the LWP and rain evaporation/production processes are positively-forced by decreasing N_{ice} . In the turbulent subsidence cases, $\delta Q_{sg}/\delta t$ does increase below cloud with increasing W_{sub} (Fig. 7A). This is the only key difference between decreasing N_{ice} and increasing W_{sub} ; therefore, increased latent heating through snow growth at cloud base – alongside heightened below-cloud rain evaporation and efficient cloud-top radiative cooling via a high LWP – is required to generate the heightened TKE (as illustrated here by w'^2) in these scenarios. Convection is suitably induced in LO- and HISUB_D10x0.5 as the modelled snow growth rates are greater (Fig. S8). Whilst the same N_{ice} is modelled in each of these scenarios, the subsidence cases produce a much colder BL than CNTRL_D10x0.5; therefore, the environmental conditions in LO- and HISUB_D10x0.5 facilitate snow growth below cloud, whilst the control produces comparatively inefficient growth conditions.”

4. It is odd to me that the authors consistently show dN_{rain}/dt to talk about increased/decreased evaporation and not dq_{rain}/dt (rate of change of rain mass). Just because there are more/fewer drops being evaporated doesn't necessarily mean that more/less rain mass is being evaporated. And it is the amount of mass that controls the latent cooling magnitude and feeds into turbulence. Showing rain mass and rain mass rates of change instead would help to strengthen their arguments. The same comment applies to snow sublimation.

- We have updated Figures 3, 5, 7, 10 and 13 to show rates of change of mass instead of number. In Figs. 5 and 7, we have kept the number concentrations of snow+graupel and rain as overlaid contours, as we feel this provides a holistic representation of how the precipitable Q-fields are changing under large-scale subsidence. This change made us realise the importance of latent heating due to snow growth at cloud base; therefore, we thank Reviewer 1 for the suggestion.

Minor Comments:

5. The title doesn't seem to reflect the content of the paper well. The below-cloud evaporation is only given as one contributing factor to the promotion of convection in these clouds. Also, it is only one aspect of the subsidence issue among many that are discussed in the text.

- The title has been changed to make a more general statement about the contents of the study:

"Relating large-scale subsidence to convection development in Arctic mixed-phase marine stratocumulus"

6. The introduction has lots of good information, but I think that it is confusing sometimes about whether the results pertain to the subtropics, Arctic, or both. Also, I find the motivation for the study a little confusing in the last paragraph of the introduction. The focus is on CAO transitions, but most of the study is not focused on CAOs. Is decreasing subsidence associated with CAO transitions? If so, this has not been clearly stated, and the link to tests 1-3 is not clearly made later.

- We had originally included a detailed overview of findings from previous studies which investigated Sc-to-cumulus transitions on a microphysical level to show the current state of knowledge. Given that little work has been done on mixed-phase clouds in a CAO, we showed results from studies of subtropical clouds. Some of these studies have suggested that subsidence may influence stratocumulus to cumulus transitions, and this finding formed part of the motivation for this work. To this end, we felt that details of these studies should be included.

We do, however, see Reviewer 1's point that this has made the Introduction misleading as we do not simulate a CAO. We cannot use our model to do this (as discussed in Sect. 4.4); we have instead used our model to identify what impact subsidence has on mixed-phase cloud microphysics on a more fundamental level. This investigation may therefore allow some inferences to be made about the role of subsidence in a CAO.

We have modified the Introduction to reflect Reviewer 1's comments; specifically, we have been clearer on whether we are discussing polar or tropical studies, and the roles of both precipitation and subsidence. We have removed some of the discussion of CAOs and streamlined what remains to make the relevance to our study much clearer. Additionally, we have added a clearer link at the end of the Introduction section (page 3, lines 3-9) as to why we have designed the experiments in this way: to demonstrate the microphysical feedbacks which are affected by subsidence and test how the combination of subsidence and a warming surface can affect BL development.

7. Page 3, Lines 13-16. So cloudiness and high pressure are correlated in subtropical marine environments, and anti-correlated in the Arctic? Why?

- This is correct, and contributed towards the motivation of this study. In subtropical marine environments, high pressure systems have been found to correlate with cloudiness due in part to the presence of a surface heat source; the ocean. Most Arctic studies consider sea ice-covered surfaces, which are devoid of this source. Arctic clouds in high pressure systems are therefore cut off from moisture sources from below (by the sea ice barrier) and above (by the subsidence and strong BL temperature inversion attributed to the high

pressure system), often leading to cloud dissipation and reduced cloud fractions. We use our experiments to show how mixed-phase clouds in Arctic marine environments may be influenced by large-scale subsidence, as this has not previously been considered in such detail. Instead of cloud dissipation, we find that the ocean surface heat source allows the clouds to behave similarly to at lower latitudes. We suggest that the reason for this is the increased inversion strength from the high pressure system (large-scale subsidence), which promotes cloudiness in these scenarios through efficient cloud top radiative cooling, below-cloud rain evaporation/snow growth, and convection development.

8. Page 5. The text describes tests 1, 2, and 4, but not test 3. The description of the control simulation should probably be given before describing the tests.

- We have re-arranged the text following Reviewer 1's comments. The control experiment is now described before the test cases (page 4, line 5-9), and text from Sect. 3.3 has been moved to the following paragraph (page 4, lines 10 - 15) to provide context for test 3.

9. Page 7, Lines 27-28. Why do non-zero snow rates implicitly suggest heterogeneity in the snow field?

- This field is averaged across the domain; therefore, if no snow reached the surface, these rates would be zero at low altitude, or largely negative to indicate significant sublimation across the domain. We realise that this is not particularly clear with the current wording; therefore, we have referenced the Z-X slices shown in the Supplement as these show the heterogeneous distribution of snow much more clearly (page 7, lines 3-5):

"Precipitation as snow does reach the surface; however, the spatial distribution becomes more heterogeneous with increased W_{sub} (not shown, Fig. S3 - S5)"

10. Figure 3. I can't tell which lines are dashed in Fig. 3f (although it's easy enough to figure out).

- We feel that both of these traces are important to show, so instead of removing the dashed Q_{tot} lines we have made them thicker and more distinct for the reader.

11. Page 9, 1st paragraph. Why higher LWP? The authors mention later that it is reduced entrainment of dry air, but that could be explicitly mentioned here.

- We were unclear on which paragraph was being referred to as the first paragraph on Page 9 does refer to the higher LWP. Upon re-reading this section, we thought it may have been the first paragraph of Sect. 3.1 that was being referenced; therefore, we have noted the stronger inversion in this paragraph alongside the initial comment regarding the increased LWP (page 6, lines 3 - 5):

"A stable Sc is modelled in the absence of W_{sub} (CNTRL, Fig. 2a). Increasing W_{sub} (LO- and HISUB) makes the temperature inversion stronger, as shown in Table 2, thus reducing entrainment into the cloud from above the BL."

12. Page 9, Lines 21-23. While I certainly agree that each individual droplet will be larger, I don't see why that necessarily means that the LWP must increase. In fact, I

would probably expect the opposite response. For lower N_{drop} , that you would get more rain production, fallout and evaporation leading to overall reduced LWP.

- Yes, for a lower N_{drop} one would expect more rain production and fallout; however, as all of our modelled rain evaporates below cloud, this moisture is retained by the system and recycled into the cloud. N_{drop} is prescribed and is therefore fixed throughout the simulation, and only the liquid mass is prognostic. Any condensed mass is automatically distributed amongst this fixed number population, and any increase in mass corresponds to an increase in size. Therefore, a lower N_{drop} corresponds to larger droplets. However, rain number and mass concentration are both represented in the model so, whilst the droplet category is limited by number, the rain category is not. This is indeed what we see, as shown by the black contours in Fig. 5B: a greater N_{rain} is modelled with $N_{\text{drop}50}$. This increased N_{rain} therefore contributes towards a greater LWP.

We realise that the inclusion of this comment is misleading without this explanation; therefore, in the interest of clarity, it has been removed.

13. Page 10, 1st paragraph. The profiles of turbulent quantities seem almost unchanged with changing N_{drop} , and the differences described are hard to see.

- We agree that these differences are small and difficult to see. We have re-ordered most of this subsection (pages 9-10) to focus less on the small changes previously discussed and more on the key messages we wish to convey. Additionally, we have re-arranged the subsequent sections in a similar manner to emphasise the key differences and not focus so much on the smaller ones.

14. Page 11, Line 3. Why would the downdrafts facilitate precipitation production? I primarily associate downdrafts with liquid evaporation and reduction of precipitation.

- Cloud top longwave cooling would produce the downdrafts consisting of colder air. These colder temperatures promote vapour growth of ice/snow crystals and condensational growth of cloud droplets in the downdraft column throughout the cloud. Additionally, the downwards motion would provide good opportunity for collision-coalescence between droplets, such that they reach precipitable sizes. Liquid evaporation and precipitation reduction would certainly occur (and does occur) toward cloud base if the particles fall below the lifting condensation level; however, we are referring to downdrafts within the cloud layer. Nonetheless, we have removed this comment in the process of tightening up the manuscript.

15. Page 11, Line 14. How is N_{drop} decreased? N_{drop} is held constant in the simulations.

- N_{drop} is prescribed and is chosen prior to running each simulation. It is this prescribed number concentration that is altered. Once the simulations are initiated, N_{drop} remains constant.

16. Page 11, Line 17. Smaller effect on N_{rain} than what?

- A smaller effect than decreasing N_{drop} . We have clarified this point in the manuscript (page 11, line 11):

“Increasing N_{drop} has a smaller effect on N_{rain} than decreasing it, as expected by the...”

17. Page 13, Lines 9-10. This sentence is confusing. Please rephrase.

- We agree that this sentence was confusing; however, we decided to remove it entirely rather than rephrasing as the point being made was extremely minor.

18. Page 13, Line 12. More exaggerated than what? The CNTRL case?

- Correct, we have clarified this in the manuscript (page 12, lines 5-6).

"... for example, the extremes in the $w'\Theta'$ profiles are more exaggerated in the LO- and HISUB cases than the CNTRL when a lower N_{ice} is modelled..."

19. Page 15, Lines 5-9. This seems like a minor detail that doesn't need to be discussed. Plus, the trends at 9hrs can't be used to understand how you arrived at the current state at 9hrs.

- We agree that this is a minor detail which has been given too much attention. In the interest of tightening up the manuscript, we have removed this segment of text, and Fig. S9.

20. Page 18, Line 1. Increased snow sublimation compared to what?

- We were referring to the fact that the $\delta N_{sg}/\delta t$ rates shown were negative <750 m in the CNTRL_SURFWARM case and <500 m in the subsidence cases, suggesting that the snow was subliming more so as it reaches the surface in this case than without surface warming. This segment of text has now been removed due to changing $\delta N_{sg}/\delta t$ to $\delta Q_{sg}/\delta t$ throughout the manuscript.

21. Page 18, Line 13. Incorrect units on TKE.

- This has been corrected to m^2s^{-2} (page 17, line 16)

22. Page 18, Lines 19-20. The discussion is repeating itself.

- This discussion has been re-located to earlier in the section; however, the ordering of this section has changed substantially on revision and therefore some re-wording has also been carried out.

23. Page 19, Lines 3-5. This sentence is confusing. Please rephrase.

- We have rephrased this sentence as requested (now page 20, lines 32-33), and added a reference to a similar figure of the CNTRL simulation included in the Supplement:

"Similarly, total ice number concentrations (ice+snow+graupel, N_{isg} , Fig. 11b) are largely unaffected by a warming surface (with comparison to Fig. S3b); however, both Q_{liq} and N_{rain} increase."

24. Page 21, Line 4. Cloud extent has never been shown. Or do you mean vertical extent? I had interpreted it as cloud fraction. I don't understand how the next sentence is a logical conclusion from this sentence.

- Reviewer 2 also raised this issue; we apologise for any confusion. We were referring to the cloud depth and indeed made a poor choice of wording. We have changed this to “cloud depth” in the manuscript (now page 19, line 6).

25. Page 22, Lines 10-25. If the focus on this section is subsidence and microphysics, then these lines are not necessary.

- We agree with Reviewer 1’s comment: lines 10-17 have been moved to Sect. 4.3, whilst lines 18-25 have been reworded into Sect. 3.1. Some of the discussion has been reworded and reworked into existing paragraphs on revision.

26. Page 26, Section 4.5. I’m not sure what this section adds to the manuscript. All of the points seem to have been made already.

- We had included this section to summarise the main points as the paper is quite detailed. We understand the reviewers concern that it is just repetition; therefore, we have removed this and ensured that the points discussed are included in the Conclusions section.

27. Page 27, Line 9. The authors have not shown that precipitation formation is enhanced in downdrafts.

- The Z-X cross sections (Figs. 11, 12) show N_{rain} as white contours on the second panel and W as shading on the bottom panel. Higher N_{rain} within the cloud layer does appear to be co-located with strong downdrafts (this is clear in Fig. 12). This was also inferred by theory, as downdrafts would create conditions for efficient collision-coalescence, allowing the droplets to grow to precipitable sizes. We have removed this statement from the Conclusions and moved it to the Discussion section (Sect. 4.2, page 20, lines 33-34), and added a reference to these figures in the manuscript as explanation of this fact.

28. Page 27, Line 12. W_{sub} cannot possibly be in a feedback loop since it is held constant in the simulations.

- We agree that this point was incorrectly made: it was our intention to state that a feedback loop between the LWP, rain evaporation, snow growth, and TKE development was positively forced by imposing greater levels of W_{sub} . Yes, W_{sub} is not part of this loop, but it makes this loop stronger. This was our intention, and we have re-worded the manuscript to reflect this (page 24, lines 27 - 30):

“The combination of strong cloud top radiative cooling, below-cloud evaporative cooling, and latent heating from snow growth at cloud base generates more TKE within the BL. These three requirements combine to form a feedback loop consisting of LWP, below-cloud rain evaporation/snow growth, and TKE development, positively forced by the magnitude of W_{sub} .”

29. Page 27, 3rd and 4th points. These points seem to mostly restate the first two conclusion points. In general, I think that the paper could be strengthened by highlighting just three or four main take-home points rather than nine.

- We agree in hindsight it was not helpful to include so many points in the Conclusion. As suggested by Reviewer 1, we have scaled this back to 4 key “take home” messages that we wish to emphasise to the reader.
-

This manuscript describes a series of simulations of mixed-phase stratocumulus clouds designed to elucidate the role of large-scale subsidence in maintaining such clouds. The main conclusion is that subsidence enhances droplet evaporation at cloud top and below the cloud base, as well as supporting the cloud top inversion. Collectively, this isolates the cloud from entrainment of dry subsiding air from above, thereby enhancing in-cloud turbulence and promoting longevity. For southward moving mixed-phase Sc, such as during cold air outbreaks, simulations suggest advection over a relatively warmer surface promotes dynamic coupling and evolution of the cloud, but stabilization under high subsidence. The manuscript is well-researched and thorough, and is well-suited for publication in Atmospheric Chemistry and Physics. I recommend that it be published after a minor revision addressing several comments below.

General Comments:

1) The manuscript is generally well-written, but it is quite long and the preponderance of details distracts from the take-home messages of each section. It is therefore difficult at times to follow. I am hoping that it can be tightened up throughout with the goal of drawing out the key points.

- Reviewer 1 also made this comment: we have tightened up the manuscript significantly following both Reviewers' comments.

2) The simulations presented appear to be based on a case study from the eastern Arctic outlined by Young et al. (2017). Terms "Arctic", "low Arctic" and "sub Arctic" are variously used and I find myself somewhat lost geographically. I feel the necessary context may lie in Fig. 2 from Young et al (2017), but it is also not clear how much of the present study is hypothetical or how closely it relates to the previous work.

- We understand that context is difficult without consulting Young et al., 2017. We use the term "Arctic" for Arctic-wide discussions and "high Arctic" for high (>80°N) latitudes typically covered in sea-ice. We have removed "sub-Arctic" and "low-Arctic" from the discussion to avoid confusion. Most of these terms are used in the literature; however, we have added these latitude ranges to the manuscript to make these locations more obvious to the reader (page 2, line 29). Additionally, we have included more in the Methods section (page 5, lines 6 - 7) relating to the setup of the model:

"..., centred on 71° in the European Arctic to allow appropriate SW radiation estimates to be calculated by the model."

3) Following on from (2), the conclusions of the study are highly generalized, which is consistent with the experimental design of the simulations, except for the fact that it is ultimately based on a single atmospheric state case at initialization, which the reader learns little about. The importance of this limitation is not clear.

- Given computational expense, we could only conduct our chosen experiments for one set of initial conditions. We understand that variation from these conditions would have been beneficial to appreciating how general our findings are. We are planning on conducting more experiments in the future; specifically, we would like to know how a neutral BL, instead of a stable one, would affect our results. Until we do more work on this, we cannot answer how

important this limitation is. Therefore, we have added more into the Discussion section to make this limitation clearer to the reader (page 21, lines 20-22).

“... This stability is likely influenced by the stable conditions used to initialise the model, and one must note that only a single set of initial conditions were used in this study.”

4) I don't understand how the model treats the surface properties and coupling, and thus to what degree dynamic coupling with the surface can feed back to the cloud, or if this can be evaluated at all (e.g., test 1 and test 4).

- The LEM computes surface fluxes from the lowest levels of the input fields (e.g. Θ , Q_{vap}). Changes in these fields through, for example, evaporative cooling from precipitation, can then be fed back into the surface levels; however, the changes are very small and the surface temperature can be assumed to remain constant in test 1. In test 4, we deliberately force Θ_{surface} as described in the text of Sect. 2.1 to produce a warming surface. This forcing produces greater heat and moisture fluxes into the model domain from the surface, which then can affect the BL structure and cloud microphysics as described in Sect. 3.4. The $w' \Theta'$ and $w' Q_{\text{vap}}'$ fluxes shown in Figs. 3 and 10 show to what extent the surface plays a role in driving the BL convection development, with little surface input shown in Fig. 3 and significant contributions in Fig. 10. The presentation and discussion of these fluxes is as far as we take the evaluation of the input of the surface.

Specific Comments:

Title: “Large-scale : : via : : :evaporation” and also enhanced cloud-top radiative cooling, right?

- Yes, this is correct. Reviewer 1 also raised this issue; therefore, we have simplified the title to: “*Relating large-scale subsidence to convection development in Arctic mixed-phase marine stratocumulus*”. This therefore does not address specific reasons and creates a broader title to encapsulate all of the physical processes discussed.

Abstract Line 20: Clarify “warming surface”, which you do not mean to be climatological, but rather southward advection.

- We have clarified this statement as requested. We have added more information closer to the beginning of the abstract when the sensitivity studies are first introduced (page 1, lines 7-8):

“... and a warming surface (representing motion southwards)...”

Page7 Line5: “an” should be “a”

- Changed as requested

Page9 Line9: For the cases that become dynamically coupled, is the surface becoming a moisture source?

- Yes, this is what we believe is happening. From Fig. 3(h), the two subsidence cases (which become dynamically coupled) have a greater upward flux of moisture from the surface and lower BL than the CNTRL simulation. The

timestep shown is 9 h, but this effect is also seen at the later times (9 - 12 h) when these cases tend towards coupling.

Page13 Lines1-6: Why the later, more rapid increase in CNTRLD10x2? Is this important somehow to understand the main thesis of this simulation?

- The reason is not entirely clear; however, we suspect it is a similar manifestation of the ice phase influencing cloud dynamics as shown in the D10 ocean case in Young et al., 2017. In summary, the higher ice number concentration modelled in the D10x2 cases may be acting to introduce localised regions of convection into these mixed-phase clouds, with hot-spots of LWP forming. The processes involved in this hypothesis are summarised in Sect. 5.2 of Young et al., 2017. We have included a summary of this discussion in the manuscript at Page 11, lines 32-33:

“The cause of this increase is not clear; however, it may be due to increased localised cloud convection caused by the high N_{ice} , which has been previously modelled by Young et al., 2017.”

Page13 Line5: “earlier” not “more quickly”?

- We agree with your suggestion and have made this change in the manuscript (now page 11, line 31).

Page13 Line7/Page27 Line13-14: This doesn't seem right. Looks like the LWP response to Nice is much larger than the response to subsidence.

- This is correct and was an error on our part. This text has been changed to better describe Fig. 6 (page 12, lines 1-3). N_{ice} does indeed affect the LWP more than W_{sub} ; however, the addition of subsidence acts to stabilise the LWP timeseries, producing stable, or even increasing, trends. This stability would help to sustain the cloud against glaciation through the WBF mechanism, whereas the decreasing LWP trends of the CNTRL simulations would be susceptible to this phenomenon.

Page15 Line23: Is the ascent of the cloud exacerbating the difference relative to CNTRL in 7B(a,d) since its spatial position is changing relative to CNTRL?

- Yes we do believe this will be a factor in the interpretation of the D10x0.5 simulations in Fig. 7B (and 7A). Subsidence acts to maintain cloud top height, as shown by the contoured number concentrations in Fig. 7A(a,d), B(a,d). Therefore, positive rain/snow production rates above approximately 1500m are not true “production”: in the LO- and HISUB cases, the production rates at these altitudes are zero, whilst they are strongly negative in the ascending CNTRL. As a result, this manifests as a positive production rate in the subsidence cases. We have included discussion of this point to ensure the reader is not misled (page 14, lines 1-5):

“Consequently, cloud top height increases in D10x0.5, while this ascent is suppressed in D10x2. This ascent adds complexity into the interpretation of Figs. 7A(a,d), B(a,d) as we are comparing clouds which are ascending at different rates. Strong cloud-top evaporation/sublimation of rain/snow is modelled above 1500m with the ascending CNTRL cloud, whilst the LO- and HISUB cases have no activity at these altitudes; therefore the anomaly between the W_{sub} and CNTRL simulations appears positive at these heights.”

Page21 Line4: Replace “extent” with “depth” or “physical thickness” so as not to be confused with horizontal extent.

- This has been changed to “depth” as requested (page 19, line 6).

~~Large-scale~~ Relating large-scale subsidence ~~promotes to~~ convection development in sub-Arctic ~~Arctic~~ mixed-phase marine stratocumulus ~~via enhanced below-cloud rain evaporation~~

Gillian Young^{1*}, Paul J. Connolly¹, Christopher Dearden¹, and Thomas W. Choullarton¹

¹Centre for Atmospheric Science, School of Earth and Environmental Sciences, University of Manchester, Manchester, UK.

*Now at: British Antarctic Survey, NERC, High Cross, Madingley Road, Cambridge, UK.

Correspondence to: Thomas W. Choullarton (choullarton@manchester.ac.uk) and Gillian Young (giyoung@bas.ac.uk)

Abstract.

Large-scale subsidence, associated with high pressure systems, is often imposed in large-eddy simulation (LES) models to maintain the height of boundary layer (BL) clouds. Previous studies have considered the influence of subsidence on warm ; liquid clouds in subtropical regions; however, the relationship between subsidence and mixed-phase cloud microphysics has not specifically been studied, ~~especially in mixed-phase clouds~~. For the first time, we investigate how widespread subsidence associated with synoptic-scale meteorological features can affect the microphysics of ~~sub-Arctic marine~~ Arctic mixed-phase marine stratocumulus (Sc) clouds. Modelled with LES, four idealised scenarios – a stable Sc, varied droplet (N_{drop}) or ice (N_{ice}) number concentrations, and a warming surface (representing motion southwards) – were subjected to different levels of subsidence to investigate the cloud microphysical response. We find strong ~~microphysical~~ sensitivities to large-scale subsidence, indicating that high pressure systems in the ocean-exposed ~~low-, or sub-,~~ Arctic regions have the potential to generate turbulence and changes in cloud microphysics in any resident BL mixed-phase clouds.

Increased cloud convection is modelled ~~within the clouds~~ with increased subsidence, driven by longwave radiative cooling at cloud top and rain evaporative cooling ~~below cloud base~~ and latent heating from snow growth below cloud. Subsidence strengthens the BL temperature inversion, thus reducing entrainment and allowing the liquid- and ice-water paths (LWP, IWP) to increase. Through increased cloud top radiative cooling and subsequent convective overturning, precipitation production is enhanced: rain particle number concentrations (N_{rain}), in-cloud rain mass production rates, and below-cloud evaporation rates increase with increased subsidence. ~~In these liquid-dominated mixed-phase clouds, subsidence contributes towards increased BL inversion strength, BL turbulent kinetic energy (TKE), and cloud LWP.~~

Ice number concentrations ~~(N_{ice})~~ play an important role, as greater concentrations suppress the liquid phase; therefore, N_{ice} acts to mediate the strength of turbulent overturning ~~induced by subsidence and longwave radiative cooling in the modelled mixed-phase clouds~~ promoted by increased subsidence. With a warming surface, a lack of – or low – subsidence allows for rapid BL TKE coupling, leading to a heterogeneous cloud layer, cloud top ascent, and cumuli formation below the Sc cloud. In these scenarios, higher levels of subsidence act to stabilise the Sc layer: ~~where~~ where the combination of these two forcings counteract one another to produce a stable, yet dynamic, Sc layer.

1 Introduction

Arctic mixed-phase clouds are long-lived, and widespread single-layer stratocumulus (Sc) decks are common in the autumn, winter, and spring. These ~~stable Sc~~ clouds are maintained and driven by convection ~~induced~~ caused by strong radiative cooling at the boundary layer (BL) inversion (e.g. Feingold et al., 2010; Morrison et al., 2012). In numerical models, mechanisms affecting the break up of these Sc clouds – including glaciation (e.g. Harrington et al., 1999; Prenni et al., 2007; Young et al., 2017) or break up into convective cumulus – (as occurs in cold-air outbreaks, ~~CAOs~~) – are often too efficient, leading to ~~inaccurate radiative predictions in the sub-Arctic region~~ radiative biases in the polar regions (Trenberth and Fasullo, 2010; Karlsson and Svensson, 2010)

Several studies (e.g. Harrington et al., 1999; Harrington and Olsson, 2001; Prenni et al., 2007; Morrison et al., 2012; de Boer et al., 2011; Young et al., 2017) have addressed the issue of premature ~~dissipation~~ glaciation of modelled mixed-phase Sc ~~through glaciation~~, often concluding that the cause is an over-active ice phase and strong influence of the Wegener-Bergeron-Findeisen (WBF) mechanism. The WBF mechanism ~~influences~~ causes a constantly changing, unstable microphysical structure ~~which often causes cloud glaciation when modelled as the represented processes are too efficient. Whilst these clouds are microphysically unstable, they can~~; however, these clouds have been observed to persist for long periods of time; ~~periods during which they may~~, and thus they have the opportunity to move geographically.

In a CAO, ~~these widespread stable Arctic~~ Sc decks are transported southwards from over the sea ice to over the warm ocean. These clouds often display closed cellular structure at first, where narrow downdraught rings surround broad updraught columns ~~to produce a cloud state which is highly reflective to incoming solar radiation (Schröter et al., 2005; Feingold et al., 2010). Similar to warm marine Sc (Kazil et al., 2014), little precipitation reaches the surface in regions of closed cellular convection. With motion southwards, increased~~ (Schröter et al., 2005; Feingold et al., 2010). Increased sensible heat fluxes and BL depth (Young et al., 2016) promote the development of precipitation through ~~induced cloud turbulence and convection (Müller and Chlond, 1996; Observations in tropical regions show that the majority of rain produced in regions of closed cellular convection evaporates below cloud (Wood et al., 2011); evaporation which has been previously shown to be instrumental in modelling the transition to open cell cumulus (Savic-Jovicic and Stevens, 2008).~~

increased cloud turbulence (Müller and Chlond, 1996). Transitions between closed and open cellular convection have been the focus of several studies (e.g. Wang and Feingold, 2009b; Feingold et al., 2010; Wood et al., 2011). Cleaner, many of which consider warm, ice-free clouds (e.g. Wang and Feingold, 2009b; Feingold et al., 2010; Wood et al., 2011). Factors controlling this transition in CAOs are poorly understood, where the mixed-phase state of the clouds adds further complexity.

In warm clouds, cleaner scenarios (with lower aerosol particle and cloud droplet number concentrations) ~~have been found to be~~ are susceptible to the formation of open cells due to ~~the resultant larger droplet sizes – through the aerosol-indirect effect – which participate efficiently in collision-coalescence interactions to form precipitation (Feingold et al., 2010; Wang and Feingold, 2009a; Rosenfeld et al., 2012)~~ efficient precipitation development (Feingold et al., 2010; Wang and Feingold, 2009a; Wood et al., 2011; Rosenfeld et al., 2012). However, ~~in subtropical marine Sc, the development of drizzle~~ drizzle formation has been found to be influenced more so by larger-scale meteorology, such as

moisture fluxes and temperature fluctuations, than aerosol-cloud interactions (Wang et al., 2010). ~~Thermodynamic interactions; Similarly in CAOs, thermodynamic interactions~~ – namely diabatic processes such as latent heat release from condensation and cloud top radiative cooling, ~~—~~ have been shown to strongly influence the broadening of convective cells ~~in CAOs~~ (Müller and Chlond, 1996; Schröter et al., 2005). Such interactions are also thought to have an important role in generating dynamical overturning in ~~both the stable the persistent~~ mixed-phase Sc upstream ~~and the closed-to-open cellular transitions downstream~~ in CAOs.

~~BL depth grows to its maximum extent at the peak of a CAO (Fletcher et al., 2016). The BL is able to grow more freely with a weaker inversion, and inversion strength can typically be related to large-scale subsidence (Myers and Norris, 2013). With less subsidence, the velocity of entrained air increases due to a greater cloud top (CT), and BL height (van der Dussen et al., 2016). Sandu and Stevens (2011) showed that decreasing the imposed large-scale subsidence in a large-eddy simulation (LES) model slows the transition from Sc to cumulus when considering warm, liquid-only clouds, as the Sc-topped layer is sustained for longer under lower levels of subsidence. As a result, the authors found that a thicker, more homogeneous Sc layer could be modelled when a lower large-scale subsidence imposed. Furthermore, recent modelling studies indicate that less subsidence extends the lifetime of sub-tropical marine Sc over a warming ocean surface and allows the liquid-water path (LWP) to increase in the absence of precipitation (van der Dussen et al., 2016). These findings suggest that synoptic-scale meteorological features have the potential to influence the microphysical evolution of marine mixed-phase Sc.~~

Regions of high surface pressure are often found upstream of CAOs in the European Arctic (Walsh et al., 2001; Fletcher et al., 2016). In the high Arctic (>80°N, over sea ice), such regions contribute towards reduced cloud fractions (Kay and Gettelman, 2009; Stramler et al., 2011). High pressure systems are associated with large-scale subsidence and, in turn, strong BL inversions (Myers and Norris, 2013). In the Arctic (over sea ice), high surface pressure anomalies — associated with anti-cyclonic circulation patterns — warm marine environments, such inversions have been shown to ~~produce less cloudy BLs (Stramler et al., 2011; Morrison et al., 2012) with comparison to cyclonic circulation patterns (Kay and Gettelman, 2009). However, in marine environments, these subsidence-enforced BL inversions lead to increased cloudiness and mixing within the BL whilst maintaining a shallow depth (Myers and Norris, 2013). Regions of high surface pressure are often found upstream of CAOs in the Arctic (Fletcher et al., 2016). Walsh et al. (2001) found that European CAOs could be linked to a negative North Atlantic Ocean (NAO) index, and positive biases in the sub-Arctic mean sea level pressure, by considering CAO climatologies over the period 1948-99. These high surface pressure anomalies are thought to be instrumental to lead to a shallow BL depth, increased cloudiness, and increased BL mixing (Myers and Norris, 2013). Previous studies suggest that large-scale subsidence may affect CAO cellular transitions (e.g. Müller and Chlond, 1996; Feingold et al., 2011) can even reduce the lifetime of liquid marine Sc modelled over a warming surface (van der Dussen et al., 2016). Subsidence associated with synoptic-scale meteorological features therefore has the potential to influence the microphysical evolution of BL clouds; however,~~ the formation of the CAO flows (Kolstad et al., 2009). With a negative NAO index, high pressure dominates in the European Arctic, moist westerly air flows are weakened, and cold air is able to move southwards towards the European continent more easily relationship between subsidence and mixed-phase cloud microphysics has not yet been studied.

The role of ~~subsidence in CAO cellular transitions has been suggested in previous studies (e.g. Müller and Chlond, 1996; Feingold et al., 2011) however, its influence on the microphysical evolution of the modelled~~ microphysics-dynamics interactions in sustaining microphy

~~sically-unstable Arctic mixed-phase clouds has not been scrutinised in detail~~ Sc is poorly understood; therefore, it is imperative to assess such feedbacks to gain a holistic view of their role in the Arctic system. By studying the cloud microphysical response to external stressors, such as large-scale subsidence, we can better evaluate the influence of environmental factors on the lifetime of mixed-phase Sc in the Arctic. Here, we investigate the ~~effect subsidence has on the microphysical stability of mixed-phase Sc clouds by considering both idealised test scenarios susceptible to the formation of precipitation and more realistic scenarios with a warming oceanic surface~~ influence of subsidence on a stable cloud, precipitating clouds, and a cloud forced by a warming surface to demonstrate how subsidence can affect a variation of microphysical scenarios common to the Arctic. By doing so, we will show which microphysical feedbacks are affected by subsidence and test how the combination of subsidence and a warming surface can affect BL development.

2 Methods

2.1 Model ~~setup~~ set-up

~~The~~ We use the UK Met Office Large Eddy Model (LEM, UK Met Office, Gray et al., 2001) to investigate the influence of large-scale subsidence on ~~marine~~ mixed-phase ~~marine~~ Sc cloud microphysics ~~is investigated using the UK Met Office Large Eddy Model (LEM, UK Met Office, Gray et al., 2001)~~. The set up is the same as that used by Young et al. (2017), whose study gives further details on the model itself. ~~The Momentum is conserved using the~~ Piacsek-Williams (PW, Piacsek and Williams, 1970) centred difference scheme ~~is used for momentum advection – conserving linear and quadratic terms to good accuracy, allowing for energy conservation (Piaeseck and Williams, 1970; Gray et al., 2001) –~~ whilst the total variation diminishing (TVD) monotonicity-preserving scheme of Leonard et al. (1993), known as ULTIMATE, is used for scalar advection (Gray et al., 2001; Shipway and Hill, 2012).

Cyclical boundary conditions and a damping layer (500 m below model lid) were imposed. Vertical profiles of potential temperature (Θ), water vapour mixing ratio (Q_{vap}), and wind speed (U and V) were implemented to initialise the model (Fig. 1): these profiles were extracted from previous LEM runs of Arctic mixed-phase Sc, specifically from 10 h in the ACC ocean case detailed by Young et al. (2017). These fields give a stable BL experiencing strong (approximately $10\text{--}15\text{ m s}^{-1}$) N-S winds. A humidity inversion, coinciding with the BL temperature inversion, ~~can be seen~~ is present in the initial Q_{vap} field (Fig. 1a): previous studies (e.g. Curry et al., 1988; Solomon et al., 2011) have shown that such inversions are often observed in the Arctic, and may act as a source of moisture to BL clouds below. Surface sensible and latent heat fluxes were calculated by the model, using near-surface Θ and Q_{vap} values, to represent an oceanic surface. The single-moment version of the Morrison et al. (2005) microphysics scheme was used, providing single-moment liquid (with a prescribed droplet number) and double-moment ice, snow, graupel, and rain.

In LES models, large-scale subsidence (W_{sub}) is often imposed as a tuning factor to maintain cloud top height. In such models, W_{sub} is usually calculated from an imposed large-scale horizontal divergence. In practice, a constant divergence is assumed below the BL temperature inversion – with zero divergence above – producing a linear increase in W_{sub} with

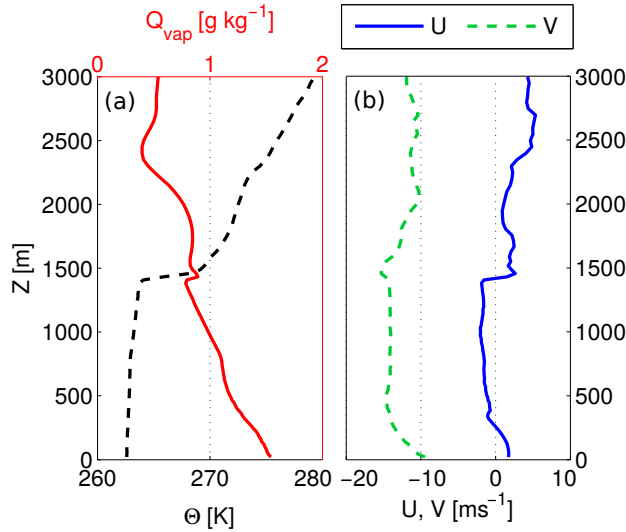


Figure 1. Profiles of potential temperature (Θ), water vapour mixing ratio (Q_{vap}), and wind speed (U , V) used to initialise the LEM.

height below the inversion, and a constant vertical wind above (Ovchinnikov et al., 2014; Solomon et al., 2015). Here, we calculate W_{sub} using this method, increasing linearly with altitude up to 1500 m. At altitudes >1500 m, $W_{\text{sub}}=W_{\text{sub}}(1500 \text{ m})$ (representing zero divergence aloft).

In the literature, the imposed horizontal divergence in LES studies often ranges from $2.5 \times 10^{-6} \text{ s}^{-1}$ (Solomon et al., 2015), through $3.75 \times 10^{-6} \text{ s}^{-1}$ (Wang and Feingold, 2009a; Feingold et al., 2015; Yamaguchi and Feingold, 2015), to $5 \times 10^{-6} \text{ s}^{-1}$ (Ovchinnikov et al., 2011). In this study, three different levels of imposed divergence – 0 s^{-1} , $2.5 \times 10^{-6} \text{ s}^{-1}$, and $5 \times 10^{-6} \text{ s}^{-1}$ – are used in four separate tests to investigate the role of large-scale subsidence in both stable and precipitation-favouring microphysical scenarios. These scenarios give an indication of how subsidence can affect the microphysics of Arctic mixed-phase clouds that remain at approximately the same latitude. Details of the tests conducted are listed in Table 1. The control simulations apply no large-scale subsidence, a prescribed droplet number concentration (N_{drop}) of 100 cm^{-3} , and use the DeMott et al. 2010 (hereafter, D10) parameterisation for primary ice nucleation. As in Young et al. (2017), an approximation of the D10 parameterisation is used, where we assume an aerosol particle number concentration of 2.20 cm^{-3} (for implementation in the parameterisation) throughout the domain.

Test 1 (Sect. 3.1) considers the effect of imposing different levels of subsidence on the microphysical properties of a stable mixed-phase Sc layer. In Sects 3.2 and 3.3, parameters relating to development of precipitation in the liquid or ice phase are varied to test the microphysical response under different levels of large-scale subsidence. For example, by decreasing droplet number concentrations (we expect to enhance rain formation by decreasing N_{drop} , See (test 2, Sect. 3.2), we expect to enhance rain formation with little effect on snow (and increase snow formation by increasing N_{ice} (test 3, Sect. 3.3). However, decreasing N_{ice} should sustain the liquid phase against the WBF mechanism, also likely affecting rain formation. Therefore, test 2). The control simulations apply no large-scale subsidence, a prescribed N_{drop} of 100 cm^{-3} , and use the DeMott et al. 2010 (hereafter,

Table 1. Simulation list.

Test number	Run label	Horizontal divergence [s ⁻¹]	Prescribed N _{drop} [cm ⁻³]	N _{ice} parameterisation	Surface forcing [Y/N]*
1	CNTRL	OFF	100	D10	N
1	LOSUB	2.5×10 ⁻⁶	100	D10	N
1	HISUB	5.0×10 ⁻⁶	100	D10	N
2	CNTRL_Ndrop50 / 150	OFF	50 / 150	D10	N
2	LOSUB_Ndrop50 / 150	2.5×10 ⁻⁶	50 / 150	D10	N
2	HISUB_Ndrop50 / 150	5.0×10 ⁻⁶	50 / 150	D10	N
3	CNTRL_D10x0.5 / 2	OFF	100	D10×0.5 / 2	N
3	LOSUB_D10x0.5 / 2	2.5×10 ⁻⁶	100	D10×0.5 / 2	N
3	HISUB_D10x0.5 / 2	5.0×10 ⁻⁶	100	D10×0.5 / 2	N
4	CNTRL_SURFWARM	OFF	100	D10	Y
4	LOSUB_SURFWARM	2.5×10 ⁻⁶	100	D10	Y
4	HISUB_SURFWARM	5.0×10 ⁻⁶	100	D10	Y

* See text for further details.

~~D10) parameterisation for primary ice nucleation. As in Young et al. (2017), an approximation of the D10 parameterisation is used, where we assume an aerosol particle number concentration of 2.20 cm⁻³ (for implementation in the parameterisation) throughout the domain. This approximation produces a relationship dependent solely on model temperature. 3 has the potential to affect both phases in the modelled clouds.~~

5 Test 4 investigates larger-scale BL interactions with a stable mixed-phase Sc layer. In CAOs, clouds move southwards off the sea ice and thus are subjected to a warming ocean surface. Model simulations in tests 1, 2, and 3 do not include any surface forcing: surface temperatures are allowed to vary through feedbacks with the BL above, yet they are not monotonically forced to become warmer. Such a forcing is applied in test 4 to investigate the combined influence of ~~imposed large-scale~~ subsidence and a warming surface, simulating motion southwards. Surface temperatures are kept constant at 263.48 K until 5 h
10 to allow adequate time for model spin up, after which they are forced to warm linearly, in hourly increments, to 265.66 K at approximately 11 h 20 min. This warming profile was artificially constructed based on approximated ERA-Interim (ECMWF Reanalysis, Dee et al., 2011) 2 m temperature variations over the ocean in the Svalbard archipelago, close to the sea ice, during a cold air outbreak (23-Mar-2013, see Young et al., 2016, 2017, and Fig. S1 for further details).

We employ a horizontal resolution of 120 m over a ~~domain of size~~ 16 km×16 km domain centred on 71°N in the European
15 Arctic to allow appropriate SW radiation calculations to be made by the model. Vertical resolution for the majority of model simulations was 20 m up to 1500 m, decreasing to 50 m between 1500 m and 3000 m (domain lid) to reduce computational cost. A second domain structure was tested to check sensitivities to this set up: the high resolution region was extended to 2300 m (again, reducing to 50 m above this height). Whilst our results are largely unaffected by the introduction of more vertical levels (not shown, see Fig. S2), this modified domain structure was applied in Sect. 3.4 (test 4) due to increasing cloud height.

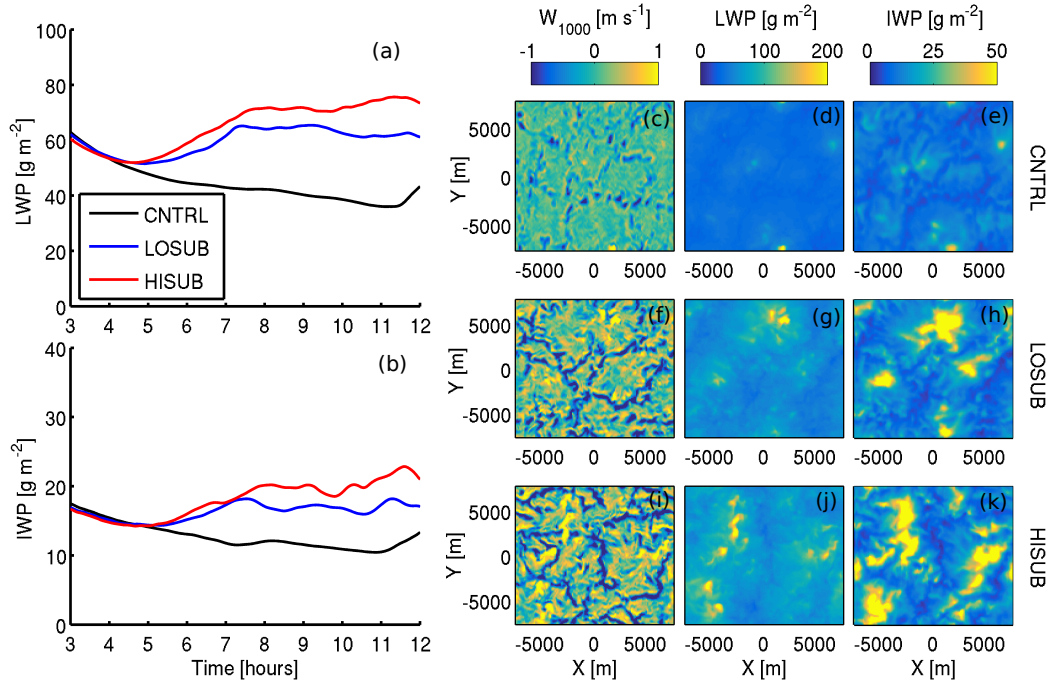


Figure 2. (a, b): Time series of the domain-averaged LWP and IWP from simulations imposing different magnitudes of large-scale subsidence. **Black:** Control cases, **blue:** low W_{sub} (LOSUB), **red:** high W_{sub} (HISUB). (c–k): Planar X–Y views of (c,f,i) vertical velocity at 1000 m (W_{1000}), (d,g,j) LWP, and (e,h,k) IWP. Planar views shown at 11 h.

3 Results

3.1 Test 1: Stable stratocumulus

Firstly, the influence of large-scale subsidence on the evolution of a stable mixed-phase marine Sc is examined. Prescribed droplet number concentrations and parameterised primary ice nucleation were not altered.

- 5 In all cases, the modelled clouds display the typical representation of ~~an~~ a liquid-topped Arctic single-layer mixed-phase Sc, with heterogeneous ice number concentrations spread throughout the cloud below (not shown, Figs. S3–S5). Domain-averaged liquid- and ice-water paths (LWP, IWP) are shown in Fig. 2(a,b), where the first 3 h of each simulation is excluded due to model spin up. A stable Sc is modelled in the absence of W_{sub} (CNTRL, Fig. 2a). Increasing W_{sub} (LO- and HISUB) ~~increases~~ strengthens the temperature inversion, as shown in Table 2, thus reducing entrainment into the cloud from above
 10 the BL. Consequently, both the LWP and the IWP increase after approximately 5 h. These traces become more variable with time when subsidence is imposed, as is particularly visible in the IWP traces, suggesting increased dynamic activity in the modelled clouds. Longwave (LW) radiative cooling is instrumental in allowing this convection to develop ~~in these clouds~~ (see Supplement, Fig. S6).

Table 2. Key BL and cloud microphysical parameters affected by large-scale subsidence in test 1. $\Delta\Theta_{il}$ is calculated across the BL inversion and is listed to illustrate the inversion strength. Peak mass sublimation/evaporation and production rates are quoted at 9 h, comparable with Fig. 3).

Run label	Peak TKE ^{a,b} [m ² s ⁻²]	$\Delta\Theta_{il}$ [K]	Peak LWP ^b [g m ⁻²]	Peak IWP ^b [g m ⁻²]	Min / Max $\delta Q_{sg}/\delta t$ [g kg ⁻¹ hr ⁻¹]	Min ^c / Max $\delta Q_{rain}/\delta t$ [g kg ⁻¹ hr ⁻¹]
CNTRL	1.0	7.52	62.9	17.5	-0.059 / 0.010	$-2.9 \times 10^{-4} / 1.3 \times 10^{-4}$
LOSUB	1.3	7.74	65.4	18.2	-0.119 / 0.025	$-5.2 \times 10^{-4} / 2.5 \times 10^{-4}$
HISUB	1.7	7.84	75.6	22.8	-0.158 / 0.041	$-8.1 \times 10^{-4} / 2.9 \times 10^{-4}$

^a At cloud top.

^b Maximum values attained within 12 h simulation time.

^c Minimum below cloud

Planar X-Y views of the vertical velocity at 1000 m (W_{1000}), LWP, and IWP fields (at 11 h), shown in (Fig. 2(c-k)), further illustrate the effect subsidence has on the spatial structure of the clouds. With increasing W_{sub} , numerous regions of high LWP/IWP develop, with heightened heterogeneity across the domain. Domain-wide variability in W_{1000} also increases with imposed subsidence W_{sub} . Broad updraught regions surrounded by narrow downdraught rings become apparent. Localised regions of high LWP and IWP can be associated with strong updraughts at 1000 m, and lower IWPs mirror the shape of the downdraught rings around the updraught regions. This locality becomes clearer with increasing W_{sub} (Fig. 2l,k).

Figure 3 illustrates the time series of total (resolved + sub-grid) turbulent kinetic energy (TKE, following Curry et al., 1988) and relative humidity (RH) shows a timeseries of TKE in panels a–c, and vertical profiles of the snow + graupel tendencies, rain tendencies, total water mixing ratio (Q_{tot}), ice-liquid potential temperature (Θ_{il}), time-averaged total vertical velocity variance (w'^2), water vapour flux ($w'Q_{vap}$) and buoyancy flux ($w'\Theta'$) key properties in panels d–i. w'^2 is used as an indicator for circulation strength, whilst the total (advected plus sub-grid) water vapour and buoyancy fluxes illustrate the mean dynamical motions in the BL. Here, a combined measure of sub-grid and advected fluxes is presented as these are of similar orders of magnitude and both make a non-negligible contribution to the flux budget (not shown, Increasing W_{sub} increases the snow+graupel mass tendencies below cloud (Fig. S7). In particular, the sub-grid $w'Q_{vap}$ fluxes are dominant in-cloud and near the surface, due to the stability of these layers.

3d). Strong snow sublimation is simulated at cloud top in all cases (Fig. 3d), with steady snow production in- and below-cloud. Increasing W_{sub} has little effect on the snow tendencies. Non-zero snow rates reach the surface, suggesting heterogeneity in the snow field across the domain. In contrast, all of the modelled rain evaporates below cloud. Regions of enhanced $\delta Q_{sg}/\delta t$ coincide with strong rain evaporation (Fig. 3e). Rain evaporation is strong at cloud top and base in all simulations; however, both the rain evaporation and production rates increase consistently with increasing W_{sub} (listed in Table 2). Heightened rain evaporation below cloud coincides with increased below-cloud BL humidity (Fig. 3b, c) and increased w'^2 in the subsidence eases (Fig. 3g); all of the rain produced evaporates below cloud and no rain mass reaches the surface. Precipitation as snow does reach the surface; however, the CNTRL simulation maintains a moist surface layer which could be acting as a source of moisture to the sub-cloud layer above it (<500 m spatial distribution becomes more heterogeneous with increased W_{sub}

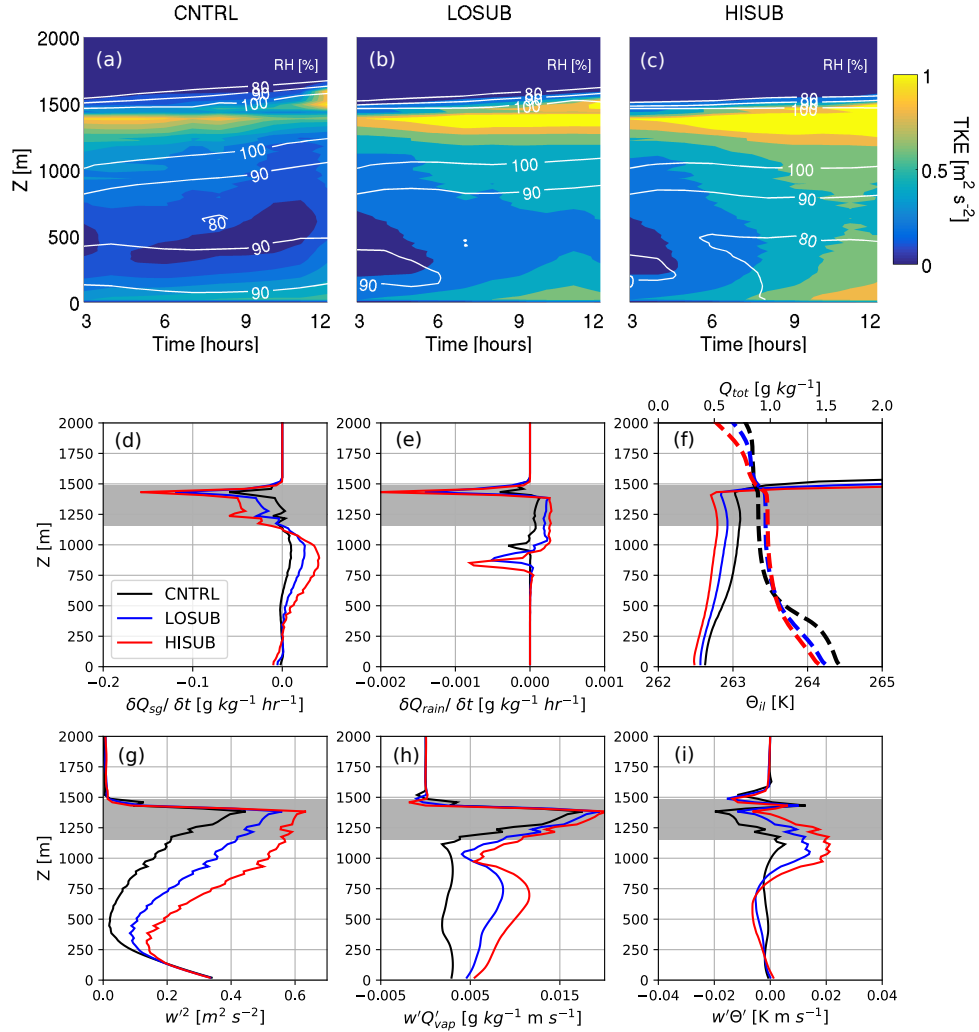


Figure 3. (a–c): Total turbulent kinetic energy (TKE, shading) and relative humidity (RH, white contours) time series for differing levels of subsidence. (d–i): Vertical profiles, at 9 h, of (d): solid precipitation (snow + graupel) mass tendency ($\delta Q_{sg}/\delta t$), (e): rain mass tendency ($\delta Q_{rain}/\delta t$), (f): ice-liquid potential temperature (Θ_{il} , solid) and total water mixing ratio (Q_{tot} , **bold** dashed) (g): vertical velocity variance (w'^2), (h): vertical flux of water vapour ($w'Q'_{vap}$) and (i): buoyancy flux ($w'\Theta'$). (g–i): w'^2 , $w'Q'_{vap}$, and $w'\Theta'$ are total quantities (sub-grid + advected). w'^2 is used as an indicator for circulation strength, whilst the total (advected plus sub-grid) water vapour and buoyancy fluxes illustrate the mean dynamical motions in the BL. A combined measure of sub-grid and advected fluxes are shown as these are of similar orders of magnitude and both make a non-negligible contribution to the flux budget (not shown, Fig. S7). In particular, the sub-grid $w'Q'_{vap}$ fluxes are dominant in-cloud and near the surface, due to the stability of these layers. Area in grey represents CNTRL cloudy regions.

(not shown, Fig. 3a). Additionally, the temperature and humidity inversion at the top of the BL acts to introduce a S3 – S5). Observational studies of Arctic mixed-phase marine Sc (Young et al., 2016) and North Atlantic CAOs (Abel et al., 2017) have previously reported precipitation as snow below cloud with little-to-no rain measured, indicating that our idealised study is in broad agreement with measurements in this region.

5 A downward flux of heat and moisture into cloud top is modelled in all cases; however, the moisture flux in particular increases slightly, caused by the temperature and humidity inversions (Fig. 3h, i): with increased levels of W_{sub} , $w'\Theta'$ increases more so in the sub-cloud layer whilst $w'Q_{\text{vap}}$ increases throughout the BL. Sub-cloud enhancement of $w'\Theta'$ coincides with the top of regions of enhanced snow+graupel mass growth (Fig. 3d). Modelled ice-liquid potential temperatures (Θ_{il} , following Tripoli and Cotton, 1981; Bryan and Fritsch, 2004) in the LO- and HISUB cases are colder than the CNTRL throughout the BL (Fig. 3f). In the region of strong rain evaporation (750 m–1200 m), below-cloud Θ_{il} tends towards an approximately neutral profile in all cases. All cases display a stable BL structure in the lower 1200 m of the BL, and an unstable structure within cloud. A minor inversion is modelled at approximately 500 m in the CNTRL case which is co-located with both a total water mixing ratio (Q_{tot}) inversion and the top of the moist surface layer in the CNTRL case.

15 Key BL and cloud microphysical parameters affected by large-scale subsidence in test 1. Minimum $\delta N_{\text{rain}}/\delta t$ values correspond to below-cloud rain evaporation, whilst $\max \delta N_{\text{rain}}/\delta t$ values relate to rain production within the cloud layer. $\Delta\Theta_{\text{il}}$ is calculated across the BL inversion and is listed to illustrate the inversion strength. Run Peak TKE^{a,b} $\Delta\Theta_{\text{il}}$ Peak LWP^b Peak IWP^b Min / Max $\delta N_{\text{rain}}/\delta t$ label $\text{m}^2\text{s}^{-2}\text{Kg m}^{-2}\text{g m}^{-2}\text{L}^{-1}\text{hr}^{-1}$ CNTRL 1.0 7.52 62.9 17.5 -7.8 / 4.3 LOSUB 1.3 7.74 65.4 18.2 -15.7 / 9.8 HISUB 1.7 7.84 75.6 22.8 -21.9 / 12.2 (Fig. 3a).

20 Subsidence acts to make the temperature inversion stronger, as shown in Table 2, thus reducing entrainment into the cloud from above the BL. TKE increases throughout the BL with increasing subsidence (Fig. 3b, c) and peaks at cloud top in all cases, likely influenced by the high evaporation and sublimations rates of rain and snow at the BL-capping temperature inversion. In all simulations, TKE typically increases with altitude through the BL. When subsidence is imposed, these TKE profiles tend towards a coupled, well-mixed BL through the top-down and bottom-up propagation of TKE. This coupling is particularly clear in the HISUB case (Fig. 3c); however, the cloud top peak in TKE remains dominant throughout every case. Therefore, increasing W_{sub} produces a more coupled, dynamic BL due to a heightened LWP, efficient LW radiative cooling, and increased rain evaporation and snow growth below cloud.

3.2 Test 2: Droplet number concentration

25 The influence of large-scale subsidence on the formation of rain in a mixed-phase marine Sc is now considered. Prescribed droplet number concentrations were varied to a lower ($N_{\text{droplet}} = 50 \text{ cm}^{-3}$) and higher ($N_{\text{droplet}} = 150 \text{ cm}^{-3}$) threshold to affect rain formation: the modelled liquid mass is distributed amongst this concentration, such that a lower (higher) concentration will yield larger (smaller) cloud drops. Therefore, we expect the lower concentration of cloud droplets to allow for more efficient rain formation. Sandu and Stevens (2011) conducted a similar sensitivity study when studying Sc-to-cumulus transitions with an LES model and found that decreasing droplet number concentrations, and enhancing precipitation, significantly affected the transition efficiency. Figure 4 shows the domain-averaged LWP and IWP for test 2, along with vertical profiles of time-averaged

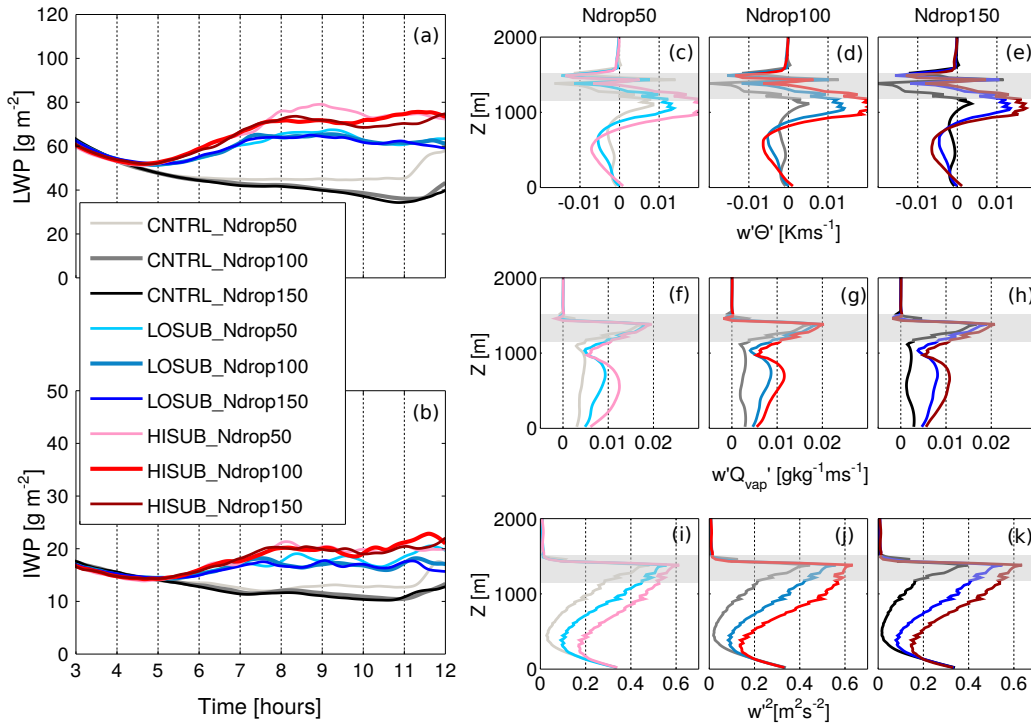


Figure 4. Domain-averaged LWP (a) and IWP (b) time series for simulations with different N_{drop} while varying the imposed large-scale subsidence W_{sub} . **Black:** Control cases, **blue:** low W_{sub} , **red:** high W_{sub} . (c-e): buoyancy flux ($w'\Theta'$), (f-h): water vapour flux ($w'Q_{\text{vap}}'$), (i-k): vertical velocity variance (w'^2). Vertical profiles shown at 9 h.

total $w'\Theta'$, $w'Q_{\text{vap}}'$, and w'^2 at 9 h. Simulations shown in variations of grey and black have no large-scale subsidence imposed. LOSUB cases are shown in variations of blue, whilst HISUB cases are shown in variations of red.

Considering the CNTRL cases, a decrease in N_{drop} allows for a slightly greater LWP to be produced (From Fig. 4a). As expected, droplets are able to grow to larger sizes and carry a greater mass as there are less sites available for condensation, producing a greater vertically-integrated liquid water mass (LWP). Modelled IWP is also greater, the Ndrop50 scenarios produce a slightly greater LWP and IWP after 8 h than the higher N_{drop} cases (Fig. 4b) Ndrop100 or Ndrop150. Increasing N_{drop} has little effect on the LWP or IWP; the results of CNTRL_the Ndrop100 and CNTRL_Ndrop150 cases are remarkably similar. Changing Additionally, changing N_{drop} has little effect on the depth of the cloud layer modelled in the CNTRL cases (shown by shading in Fig. 4c-k). Decreasing N_{drop} dynamically influences the modelled cloud by producing a greater $w'\Theta'$ within, and below, the cloud layer, suggesting a net upward flux of warm air (Fig. 4c-e). Below approximately 1000m, all CNTRL simulations display a cooling profile, coinciding with a positive upward flux of water vapour. As with test 1, the vapour profiles of all cases are influenced by the downward flux of warm, moist air from above the inversion. Turbulent activity is greater throughout the BL when less droplets are prescribed (CNTRL_Ndrop50, Fig. 4i), whereas the w'^2 profile

is dominated by sharp peaks at the surface and at the top of the BL when more droplets are modelled (CNTRL_Ndrop150, Fig. 4k).

As with test 1, greater LWPs and IWPs are modelled with increasing W_{sub} . In general, varying W_{sub} affects the modelled LWP and IWP less than varying N_{drop} (Fig. 4a,b). The LO and HISUB simulations are again more dynamic throughout the BL than the CNTRLs (Fig. 4i-k). w'^2 increases with height throughout the BL with increasing W_{sub} —excluding a minimum modelled at approximately 500 m in each case—and a greater $w'Q_{\text{vap}}$ is modelled below cloud. Peak in-cloud water vapour fluxes are largely unchanged with W_{sub} (W_{sub} , IWP, and dynamical fluxes more than the microphysical changes (varying N_{drop} , Fig. 4e-ea-i). A more substantial difference can be identified in the buoyancy profiles: $w'\Theta'$ is much greater within cloud, and more negative below approximately 750 m, than the corresponding CNTRL simulations. This positive $w'\Theta'$ is likely due to a downward flux of cold air, suggesting these cases are dominated by strong downdraughts; downdraughts which likely facilitate precipitation production.

Figure 5 shows the mass production and sublimation/evaporation rates of snow+graupel and rain relative to the CNTRL in panels A and B respectively. Absolute domain-averaged number concentrations from each subsidence simulation are overlaid as contours. Varying N_{drop} has only a minor effect on the time evolution of $N_{\text{s+g}}$. With increasing subsidence, $N_{\text{s+g}}$ decreases slightly in, and increases below, cloud. Similarly, snow the snow+graupel number concentration (N_{sg}). Snow mass production rates (relative to the CNTRL) are greater in and directly below the cloud layer increase towards cloud base and below cloud with increasing W_{sub} , whilst snow sublimation rates at cloud top also increase. Non-zero snow concentrations reach the surface in all simulations (Fig. 5A).

Figure 5B shows a contrasting trend for rain production and evaporation. As with test 1, strong rain evaporation at cloud top and base is offset by high production rates within the cloud layer. Decreasing N_{drop} strongly affects N_{rain} as expected; for example, the rain number concentration N_{rain} increases by approximately 409 L^{-1} between the HISUB_Ndrop100 and HISUB_Ndrop50 cases. For the LOSUB comparison, N_{rain} increases by approximately 6 L^{-1} in cloud. Increasing W_{sub} therefore increases the number concentration of rain particles enhances the N_{rain} produced by decreasing N_{drop} in the modelled cloud. The moist, cool sub-cloud layer and increased $w'^2 \delta Q_{\text{sg}}/\delta t$ at cloud bases shown in Fig. 4 coincide with the top of these regions of increased rain evaporation below cloud in all subsidence cases, relative to the CNTRLs, does not change significantly when changing N_{drop} , even with strengthened rain mass evaporation in this region; however, the below-cloud enhancement of $\delta Q_{\text{sg}}/\delta t$ by increasing W_{sub} is apparent in each case.

Increasing N_{drop} has a smaller effect on N_{rain} than decreasing it, as expected by the thermodynamic indirect effect; with more droplets available, droplet size decreases due to less competition for water vapour. N_{rain} decreases in Ndrop150 with respect to the Ndrop100 or Ndrop50 cases, and the in-cloud mass production and below-cloud evaporation rates are smaller. Despite this, increasing W_{sub} still increases the marginally increases the mass production/evaporation rates with respect to the CNTRL_Ndrop150 case.

No rain reaches the surface in any of these simulations; all of the N_{rain} produced evaporates directly below cloud. This evaporation effect increases with increasing subsidence; for example, the HISUB_Ndrop50 case evaporates at $-68 \text{ L}^{-1} \text{ hr}^{-1}$ below cloud at 9h. From these simulations, we suggest that the level of imposed large-scale subsidence can significantly affect

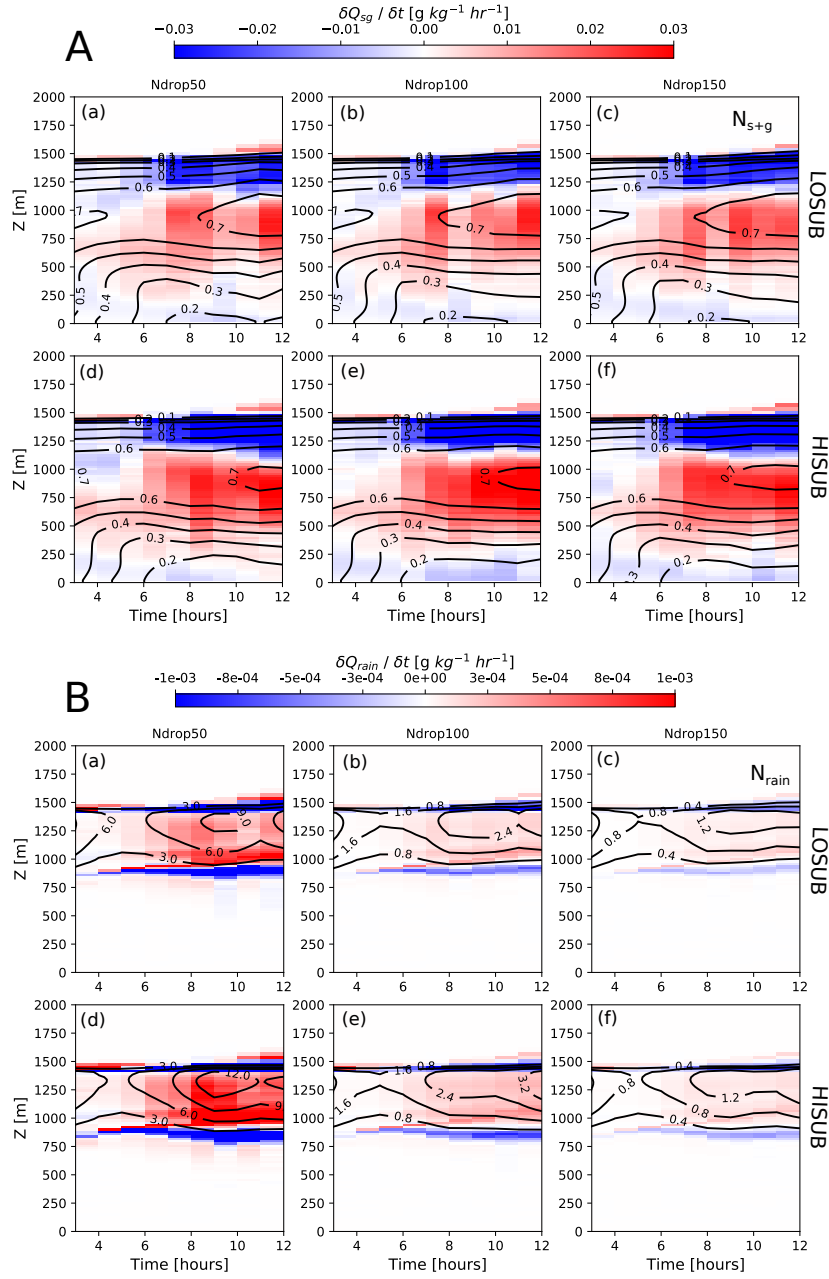


Figure 5. A: Change in $\delta N_{s+g} / \delta Q_{s+g} / \delta t$ [$\text{L g kg}^{-1} \text{hr}^{-1}$] (shading) between subsidence cases and the corresponding CNTRL simulation for test 2. Red corresponds to increased production, whilst blue shows increased sublimation than the associated CNTRL. N_{s+g} [L^{-1}] is shown as contours. **B:** As panel A, instead the change in $\delta N_{\text{rain}} / \delta t$ [$\text{L g kg}^{-1} \text{hr}^{-1}$] is shown with N_{rain} [L^{-1}] as contours. (a-c): LOSUB, (d-f): HISUB.

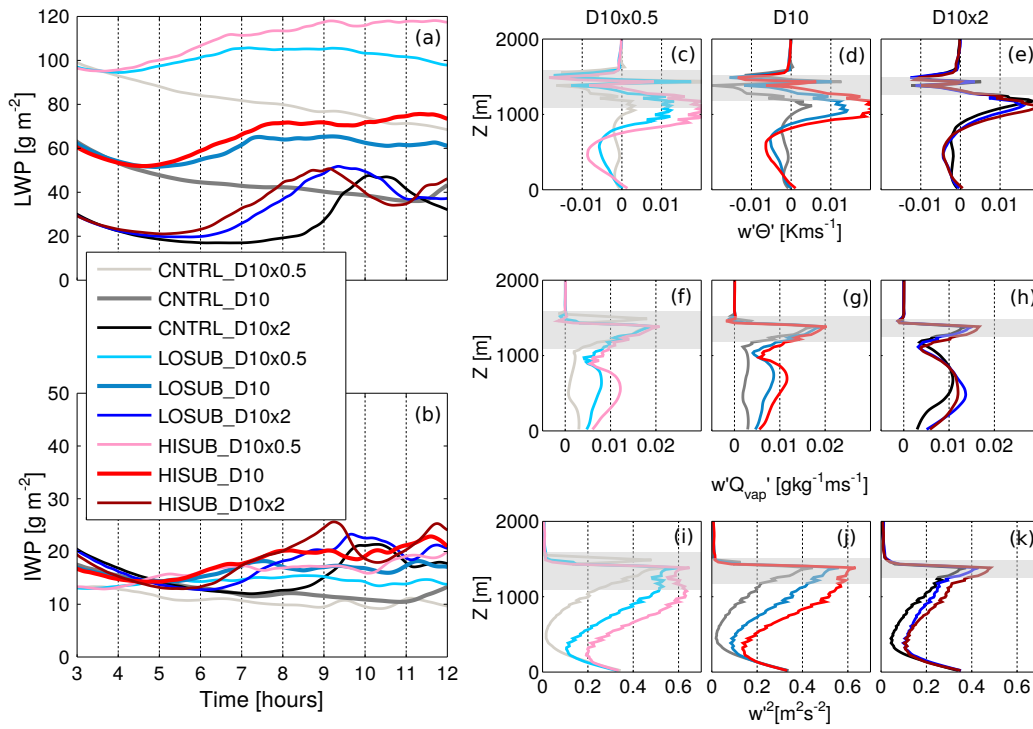


Figure 6. As Fig. 4, but with changing ice number concentrations.

the liquid phase in clean mixed-phase Sc, as W_{sub} positively forces the rain mass production/evaporation rates modelled in these precipitation-favouring microphysical scenarios.

3.3 Test 3: Ice number concentration

The influence of W_{sub} on a mixed-phase marine Sc when changing ice number concentrations is now considered. Heterogeneous primary ice formation is represented using the D10 parameterisation with aerosol number concentrations calculated during the study by Young et al. (2017). ~~Several previous~~ Previous studies (Harrington et al., 1999; Harrington and Olsson, 2001; Prenni et al., 2007; Morrison et al., 2012; de Boer et al., 2011; Young et al., 2017) have shown that the lifetime of spring-time single-layer mixed-phase clouds at high latitudes is strongly dependent on N_{ice} . Here, a lower ($N_{\text{ice}} = \text{D10} \times 0.5$) and higher ($N_{\text{ice}} = \text{D10} \times 2$) threshold are implemented to change the number concentration of modelled ice, and snow, particles.

~~We expect increasing N_{ice} to increase $N_{\text{s+g}}$, as the cold temperatures will allow for efficient vapour growth of ice particles into snow at the expense of the cloud liquid phase by the WBF mechanism. However, decreasing N_{ice} should sustain the liquid phase against the WBF mechanism, likely affecting rain formation. Therefore, this test has the potential to affect both rain and snow in the modelled clouds.~~

Fig. 6 illustrates the domain-averaged LWP and IWP for test 3. The CNTRL cloud layer – as shown by the shaded area in Fig. 6(c-k) – becomes shallower with increasing N_{ice} . When no subsidence is imposed (CNTRL, black/grey lines Fig. 6a), decreasing N_{ice} increases the LWP as expected through the influence of the WBF mechanism, whereas increasing N_{ice} has the opposite effect (black/grey lines, Fig. 6a). However, in CNTRL_D10x2, both the LWP and IWP increase sharply after 9 h (Fig. 6a,b). This LWP peak occurs more quickly earlier with increasing W_{sub} (as shown by the blue and brown traces in Fig. 6a) and, although the shape of the peak changes, this trend can also be seen in the IWP traces. The cause of this increase is not clear; however, it may be due to localised cloud convection caused by the high N_{ice} , which has been previously modelled by Young et al. (2017).

As with tests 1 and 2, the modelled LWP increases with increasing W_{sub} . Trios can be easily identified in Fig. 6(a), where increasing the subsidence decreasing N_{ice} affects the LWP more so than altering W_{sub} . Although the key factor influencing the LWP is N_{ice} . Imposing subsidence produces, W_{sub} acts to produce LWPs which are stable, or even increase, with time. Furthermore, increasing the subsidence whilst altering N_{ice} marginally increases the modelled IWP. In contrast, the CNTRL simulations typically produce a decreasing trend (with the exception of the D10x2 scenario).

W_{sub} affects the modelled fluxes (Fig. 6bc-k) ; however, the traces are similar between the varying N_{ice} and subsidence scenarios tested.

Coinciding with these larger LWPs, below-cloud w'^2 increases with increasing subsidence and decreasing more so than altering N_{ice} . Additionally, the extremes in the modelled $w'\Theta'$ profile are more exaggerated in the LO- and HISUB cases. The ; however, the exception to this trend is the high ice N_{ice} (D10x2) simulations, as subsidence does not affect this microphysical scenario as strongly as in the D10x0.5 cases. The modelled clouds are less dynamic with a larger $N_{stimulate}$ this scenario as clearly as the other microphysical scenarios shown. Despite this, there are some notable differences in the flux profiles: for example, the extremes in the $w'\Theta'$ profiles are more exaggerated in the LO- and HISUB cases than the CNTRL when a lower N_{ice} ; w'^2 becomes dominated by cloud top and surface peaks in the CNTRL_D10x2 case, similar to CNTRL_Ndrop150 in test 1. is modelled (Fig. 6c-e). These comparisons suggest that W_{sub} has can have a strong dynamical effect on liquid-dominated mixed-phase clouds, but have little influence in its influence on those with more ice. With less ice (D10x0.5), the w'^2 peak at cloud top grows larger and deeper in comparison to the D10x2 simulations, indicating that a more dynamic cloud-topped BL is modelled when less ice is present is limited.

N_{s+g} From Fig. 7A, N_{sg} increases with increasing N_{ice} as expected, and decreases only slightly between the LO- and HISUB cases (Fig. 7A). Whilst the absolute number concentrations marginally decrease, the in-cloud snow production rates – relative to the CNTRL simulations – increase with increasing subsidence, with up to $1 L^{-1} hr^{-1}$ at 12 h (1000 m) modelled in the HISUB_D10x2 case (Fig. 7A(f)). Additionally, snow mass sublimation rates at cloud top and below cloud typically increase with increased W_{sub} , similar to test 2.

As with tests 1 and 2, non-zero N_{s+g} reaches the surface (Fig. 7A), whilst all rain evaporates in the sub-cloud layer (Fig. 7B). LOSUB. The increase in LWP and IWP in CNTRL_D10x2 actually produces a greater N_{rain} at approximately 9 at 9–10 h than LOSUB_D10, whereas the HISUB cases produce less rain with increased N_{ice} as expected. This LOSUB_D10x2 artefact likely

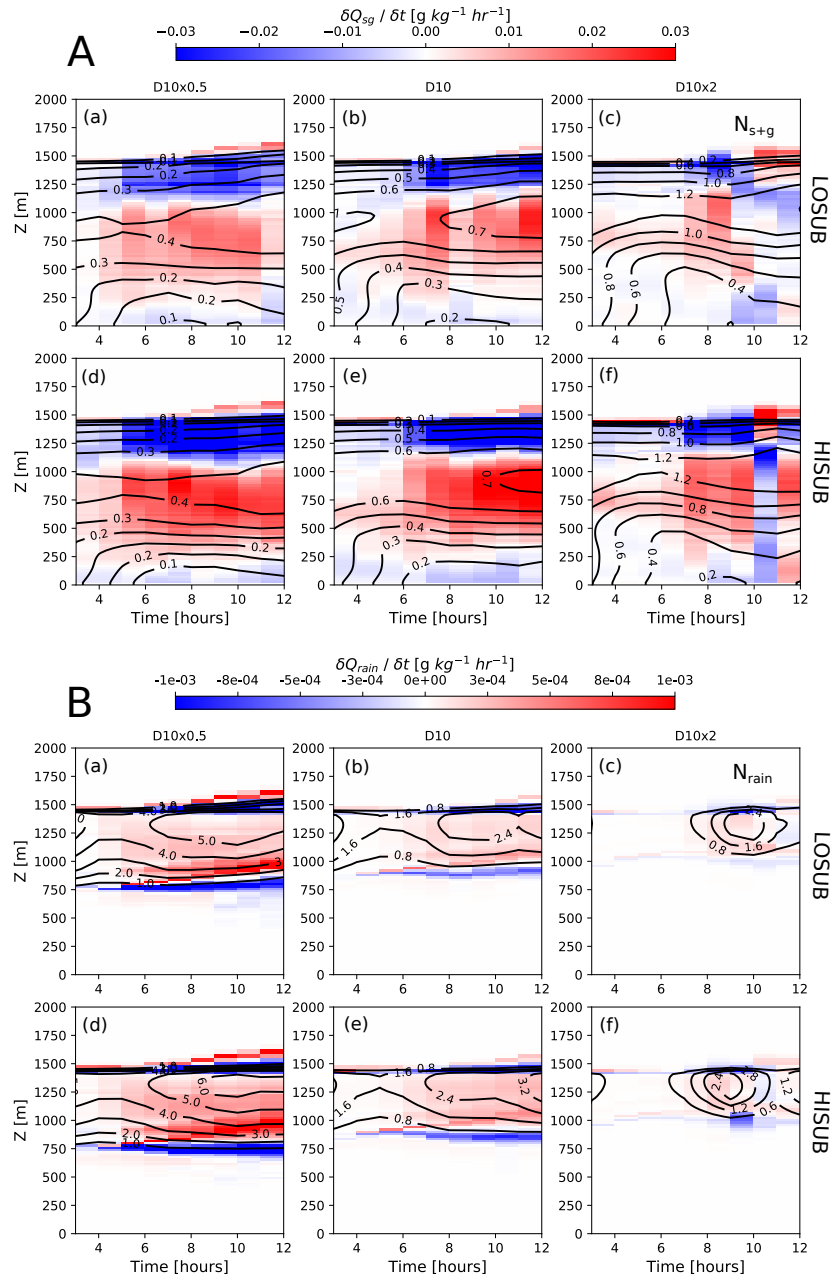


Figure 7. As Fig. 5, instead the ice number concentration is varied (test 3).

occurs due to the lower below-cloud rain evaporation rates than LOSUB_D10, and similar in-cloud production rates, allowing more rain to remain in the less-dynamic cloud (not shown, Fig. ??).

In test 2, increasing W_{sub} dynamically stimulated a scenario with inefficient precipitation production (HISUB_Ndrop150). Interestingly, W_{sub} does not have this same effect here when increasing N_{ice} ; increasing W_{sub} does not efficiently generate convection in LO- and HISUB_D10x2, and the modelled $\delta N_{\text{rain}}/\delta t$ rates vary little in comparison to the D10x0.5 and D10 cases. The consistency between affects our comparison, as increased snow mass is modelled at this time; therefore, the LO- and HISUB_D10x2 cases is also demonstrated in the small difference between the $w'\Theta'$, $w'Q_{\text{vap}}'$, and w'^2 profiles at 9h (Fig. 6e, h, k). Increasing N_{ice} appears to suppress the formation of N_{rain} by acting as a sink for water vapour and causing droplet evaporation (via the WBF mechanism), thus suppressing rain-driven convection.

simulations produce less snow mass relative to the baseline.

Greater LWPs are produced with less ice, as more liquid mass is able to form in the vicinity of ice crystals, producing larger droplets (for a fixed N_{drop}). With larger droplets, more efficient rain production can take place. Efficient rain mass production takes place with a lower N_{ice} , as shown in Fig. 7B. Rain production and evaporation rates increase strongly with increasing W_{sub} , due to the greater liquid mass being distributed over a fixed N_{drop} . $\delta Q_{\text{rain}}/\delta t$ increases with W_{sub} in the D10x0.5 case. Below-cloud In-cloud mass production and below-cloud rain evaporation rates increase with decreased N_{ice} — $40 \text{ L}^{-1} \text{ hr}^{-1}$ at 12h (700m) in the in LO- and HISUB_D10x0.5 case — relative to CNTRL_D10x0.5, as do the in-cloud production rates and N_{rain} snow growth rates below cloud (Fig. 7). With less ice available, more liquid droplets may form and grow against a weaker WBF mechanism. Cloud-cloud top radiative cooling becomes more efficient due to a heightened liquid fraction (Fig. 6a), vigorous turbulence increased rain formation (Fig. 67iB(d)), and rain formation efficient snow growth (Fig. 7BA(d)) and vigorous turbulence (Fig. 6i). Consequently, cloud top height increases in D10x0.5, while this ascent is suppressed in D10x2. This ascent adds complexity into the interpretation of Figs. 7A(a,d), B(a,d) as we are comparing clouds which are ascending at different rates. Strong cloud-top evaporation/sublimation of rain/snow is modelled above 1500 m with the ascending CNTRL cloud, whilst the LO- and HISUB cases have no activity at these altitudes; therefore the anomaly between the W_{sub} and CNTRL simulations appears positive at these heights.

LWP and below-cloud rain evaporation are enhanced in CNTRL_D10x0.5 with comparison to CNTRL_D10 and CNTRL_D10x2; however, w'^2 is not strongly affected (Fig. 6). Figure 8 shows $\delta Q_{\text{sg}}/\delta t$ and $\delta Q_{\text{rain}}/\delta t$ at 9h to illustrate differences between the D10x0.5, D10, and D10x2 CNTRL cases. $\delta Q_{\text{sg}}/\delta t$ is similar in the D10 and D10x0.5 simulations, whilst the LWP and rain evaporation/production processes are positively-forced by decreasing N_{ice} . In the turbulent subsidence cases, $\delta Q_{\text{sg}}/\delta t$ does increase below cloud with increasing W_{sub} (Fig. 7A). This is the only key difference between decreasing N_{ice} and increasing W_{sub} ; therefore, increased latent heating through snow growth at cloud base – alongside heightened below-cloud rain evaporation and efficient cloud-top radiative cooling via a high LWP – is required to generate the heightened TKE (as illustrated here by w'^2) in these scenarios. Convection is suitably induced in LO- and HISUB_D10x0.5 as the modelled snow growth rates are greater (Fig. S8). Whilst the same N_{ice} is modelled in each of these scenarios, the subsidence cases produce a much colder BL than CNTRL_D10x0.5; therefore, the environmental conditions in LO- and HISUB_D10x0.5 facilitate snow growth below cloud, whilst the control produces comparatively inefficient growth conditions.

w'^2 is greatest with the LO- and HISUB_D10x0.5 simulations (Fig. 6i) due to the dynamical activity produced dynamical stimulation by the heightened rain evaporation-mass evaporation and snow mass production at cloud base (Fig. 7B), and this

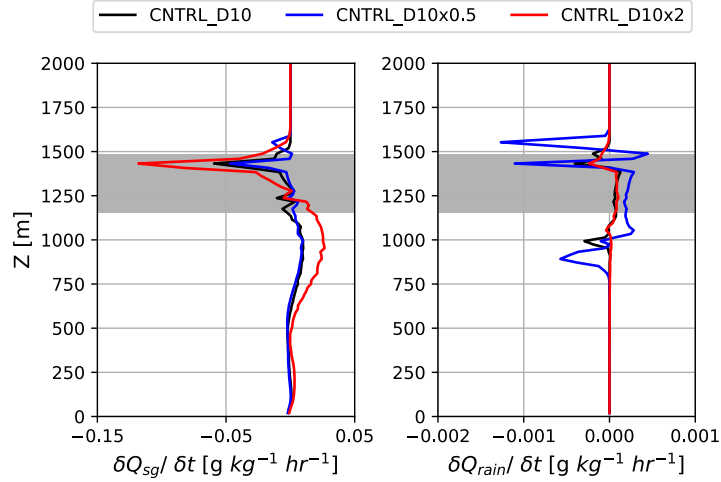


Figure 8. Microphysical tendencies comparison of CNTRL_D10, CNTRL_D10x0.5, and CNTRL_D10x2. Vertical profiles, at 9 h, of solid precipitation (snow + graupel) mass tendency ($\delta Q_{sg}/\delta t$) and rain mass tendency ($\delta Q_{rain}/\delta t$) are shown. Area in grey represents CNTRL_D10 cloudy regions.

effect is strengthened. The clouds are more dynamic with increasing W_{sub} . These conclusions support the findings of test 2, as, and it is the liquid-dominated (D10x0.5) clouds which are vulnerable to dynamic stimulation by imposing large-scale subsidence more vulnerable to this dynamic stimulation. Clouds with greater ice number concentrations N_{ice} suppress the liquid phase; therefore, the ice number concentration N_{ice} has a key role in mediating the strength of turbulent overturning generated in the mixed-phase clouds.

3.4 Test 4: Surface warming

As described in Sect. 2, our previous tests consider scenarios that would elicit a microphysical response whilst keeping the surface boundary conditions approximately constant. These scenarios give an indication of how subsidence can affect precipitation formation in mixed-phase clouds that remain at approximately the same latitude. Tests 1–3 are idealised and are not representative of the environmental forcings encountered when these clouds move southwards: observations show a sharp near-surface air temperature gradient in CAO flows transitioning southwards from the cold sea ice to the warm ocean. To address this, we further consider the combined dynamical impact of large-scale subsidence and a warming surface on both the BL and cloud microphysical structure. Whilst our domain size is not appropriate to resolve the explicit transition from closed to open cellular convection far downstream in a CAO, we will show how large-scale subsidence influences the microphysical stability of a stable mixed-phase marine Sc over a warming surface, upstream from this strong cellular convection.

The simulated clouds become more convective. More convection is modelled with time under the destabilising conditions of a warming surface (Fig. 9). This process is gradual when subsidence is imposed, as shown by the approximately monotonic increase in LWP and IWP with time; however, Domain-averaged LWPs and IWPs are similar in the subsidence cases,

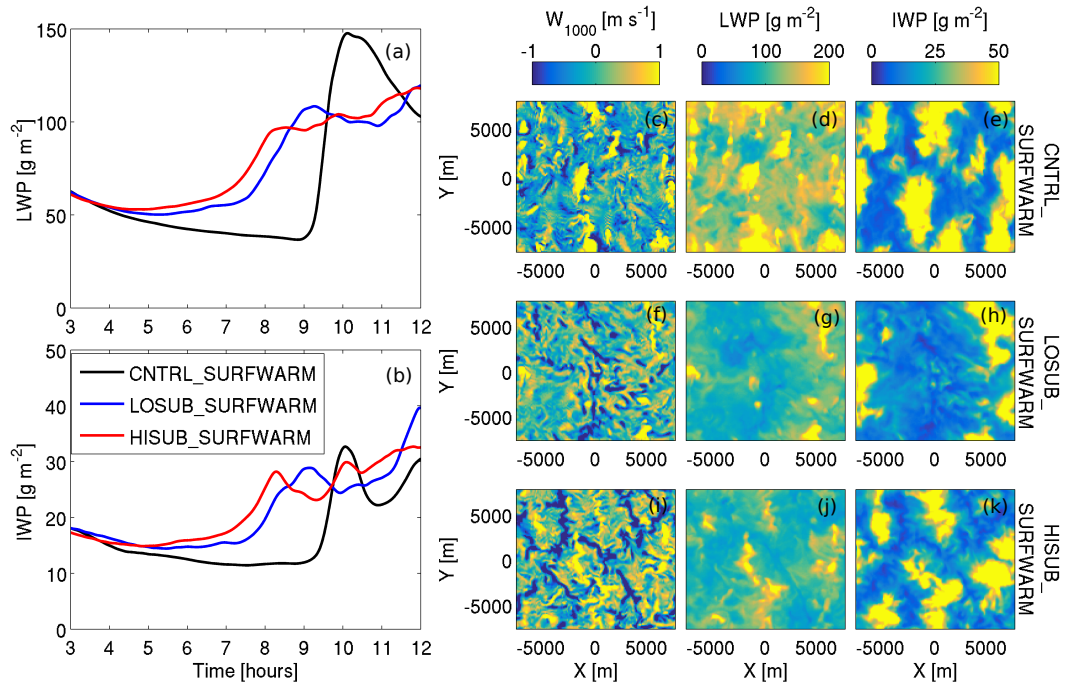


Figure 9. As Fig. 2, with the addition of a warming surface (test 4). Planar views (c-k) are shown at 10 h to capture the bulk cloud structure coinciding with the CNTRL_SURFWARM peak in LWP and IWP shown in panels a and b.

increasing almost monotonically with time (Fig. 9a,b). Slightly greater LWPs are modelled in HISUB_SURFWARM than in the LOSUB counterpart. Subsidence acts to produce greater LWPs and IWPs than the CNTRL up to approximately 10 h, at which point CNTRL_SURFWARM undergoes a significant convective transformation marked by a sharp increase in both LWP and IWP is modelled in the CNTRL_SURFWARM case at 10 h. The planar Planar views of Fig. 9(c-e) show that, at this time, the CNTRL_SURFWARM cloud contains numerous regions of very high LWP ($>200 \text{ g m}^{-2}$) and IWP ($>50 \text{ g m}^{-2}$) co-located with strong updraughts at 1000 m. The differences between the LO- and HISUB cases are not as prominent as without surface forcing (test 1, Fig. 2); however, in agreement with the test 1 simulations, subsidence again causes an increase in both LWP and IWP with time, and produces greater values than CNTRL_SURFWARM until 9 h when the control undergoes a significant convective transformation.

Figure 10 mirrors the format of Fig. 3 to allow a direct comparison of the influence of a warming surface; however, TKE data are shown over a greater colour range in Fig. 10(a-e). In contrast to Fig. 3, cloud Cloud top and surface sources of TKE couple in all cases (Fig. 10a-c). The CNTRL case couples rapidly at approximately 10 h (Fig. 10a), coincident with the peak in LWP and IWP shown in Fig. 9(a,b). Cloud top and surface TKE sources then appear to decouple at approximately 11 h. Within approximately 1.5 h, the two TKE sources decouple again. Cloud top and surface sources of TKE again separately dominate the LO- and HISUB_SURFWARM profiles separately from approximately 7 h onwards; however, the surface contributions are

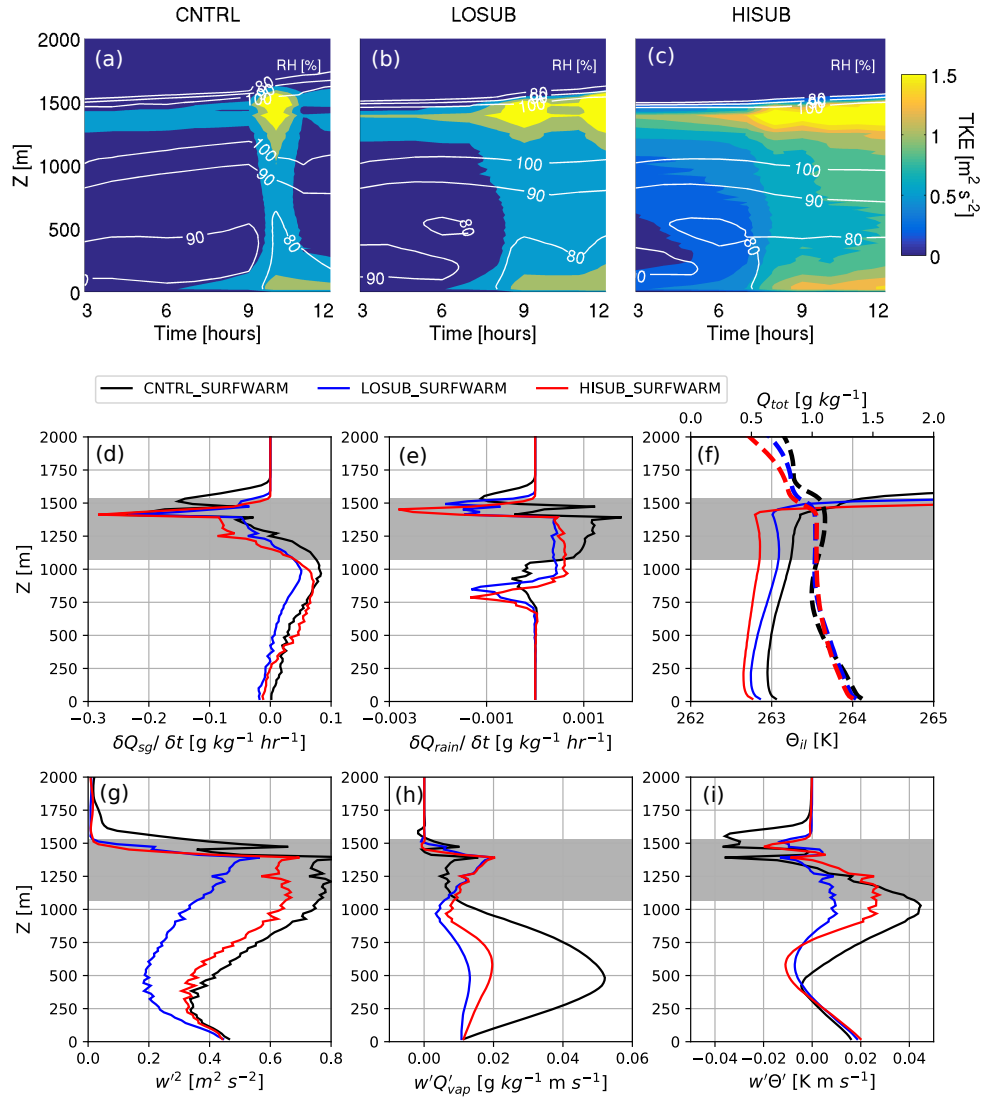


Figure 10. As Fig. 3, with the addition of a warming surface (test 4). Note the different colour scale in panels a–c, and extended x-range over which data is shown in [panel e](#) and [panels d–i](#), with comparison to Fig. 3. Vertical profiles (panels d–i) are shown at 10 h.

~~stronger than modelled in test 1.~~ LOSUB_SURFWARM displays a similar coupling at 10h to CNTRL_SURFWARM, yet it remains coupled afterwards and undergoes a second TKE burst between 11 h and 12 h. TKE ~~evolves similarly~~ evolution in HISUB_SURFWARM as in HISUB (test 1, Fig. 3e), with the propagation of SURFWARM is more gradual than the CNTRL and LOSUB cases: the top-down and bottom-up TKE gradually increasing propagation of TKE steadily increases with time to

Table 3. Key BL and cloud microphysical parameters affected by large-scale subsidence in test 6. ~~As Table 2, minimum $\delta N_{\text{rain}}/\delta t$ values correspond to below-cloud rain evaporation~~ 4. Mass tendencies are quoted at 10 h, whilst max $\delta N_{\text{rain}}/\delta t$ values relate to rain production within the cloud layer comparable with Fig. 10.

Run label	Peak TKE ^{a,b} [m ² s ⁻²]	$\Delta\Theta_{\text{il}}$ [K]	Peak LWP ^b [g m ⁻²]	Peak IWP ^b [g m ⁻²]	Min / Max $\delta N_{\text{rain}}Q_{\text{sg}}/\delta t$ [g kg ⁻¹ hr ⁻¹]	Min ^c / Max $\delta Q_{\text{rain}}/\delta t$ [g kg ⁻¹ hr ⁻¹]
CNTRL	2.8	7.63	147.7	32.7	-10.2 <u>-0.266</u> / 30.6 <u>0.083</u>	-4.8×10^{-4} / 1.8×10^{-3}
LOSUB	3.9	8.06	119.8	39.6	-20.2 <u>-0.234</u> / 16.3 <u>0.051</u>	-1.3×10^{-3} / 4.5×10^{-4}
HISUB	2.3	8.37	118.3	32.7	-31.6 <u>-0.284</u> / 21.5 <u>0.071</u>	-1.3×10^{-3} / 6.6×10^{-4}

^a At cloud top.

^b Maximum values attained within 12 h simulation time.

^c Minimum below-cloud.

couple the separated cloud and surface sources. ~~The warming surface acts to produce an instability in each of the Θ_{il} profiles at the surface (Fig. 10f).~~

~~Increased snow sublimation is modelled towards the surface in the surface warming cases (Fig. 10d), especially when subsidence is imposed.~~ Cloud top height increases steadily in CNTRL_SURFWARM (Fig. 10a), whilst this ascent is strongly suppressed in HISUB_SURFWARM (Fig. 10c) and marginally suppressed in LOSUB_SURFWARM (Fig. 10b). Negative $w'\Theta'$ fluxes at cloud top again suggest entrainment of warm air into the cloud layer from above the BL in each case; however, this flux is stronger in CNTRL_SURFWARM than in the subsidence cases, indicating that greater entrainment rates are accompanying the cloud top ascent. ~~Below-cloud and surface $w'Q_{\text{vap}}$ and $w'\Theta'$ fluxes are stronger than in test 1, likely due to the increased turbulent overturning generated by the warming surface.~~

10 ~~Qualitatively, the trends identified in test 1 remain true with a warming surface: below-cloud rain evaporation (Fig. 10e), BL TKE (Fig. 10b,c), w'^2 (Fig. 10g), and inversion strength (Table 3) are enhanced with increasing W_{sub} . However, the linearity between Significantly larger values of $w'Q_{\text{vap}}$ and $w'\Theta'$ with increasing W_{sub} shown in test 1 does not hold true in this scenario: namely, significantly larger values are modelled below cloud in the CNTRL_SURFWARM simulation (0.052 g kg⁻¹ m s⁻¹ and 0.045 K m s⁻¹, respectively) ~~are modelled below cloud in the CNTRL_SURFWARM simulation~~ than
15 in the subsidence cases, coinciding with the rapid BL coupling shown in Fig. 10(a). Convective activity increases at this time, with w'^2 increasing up to 0.90 m² s⁻² in cloud alongside a peak (cloud top) TKE of 2.8 m² s⁻² (Table 3). ~~Rain production is particularly strong~~ Additionally, rain mass production is enhanced in CNTRL_SURFWARM ~~at this time (Table 3);~~ however, below-cloud rain evaporation is still weaker than in the LO- and HISUB_SURFWARM simulations. ~~Similar to test 1, rain~~ Rain evaporative cooling below cloud in LO- and HISUB_SURFWARM ~~again~~ acts to decouple the surface and in-cloud heat
20 sources from each other (Fig. 10i); ~~however, the addition of a surface heat source causes~~. As a result, the $w'\Theta'$ profiles ~~to swing through greater extremes; for example, swing through significant extremes below cloud:~~ from 0.021 K m s⁻¹ through -0.011 K m s⁻¹ to 0.028 K m s⁻¹ in the HISUB_SURFWARM case.~~

Furthermore, the warming surface produces an unstable Θ_{il} profile at the surface in each simulation (Fig. 10f).

Z-X slices for the CNTRL_SURFWARM case at 10 h. **Top row:** total ice mass mixing ratio (Q_{isg} , shading) and liquid water mass mixing ratio (Q_{liq} , contours). **Middle row:** total ice number concentration (N_{isg} , shading) and rain number concentration (N_{rain} , contours). **Bottom row:** vertical velocity (W , shading) and relative humidity (RH, contours). Identified detached below-cloud cumuli are highlighted by red ellipses, and cumuli merged with the Sc are indicated by white ellipses.

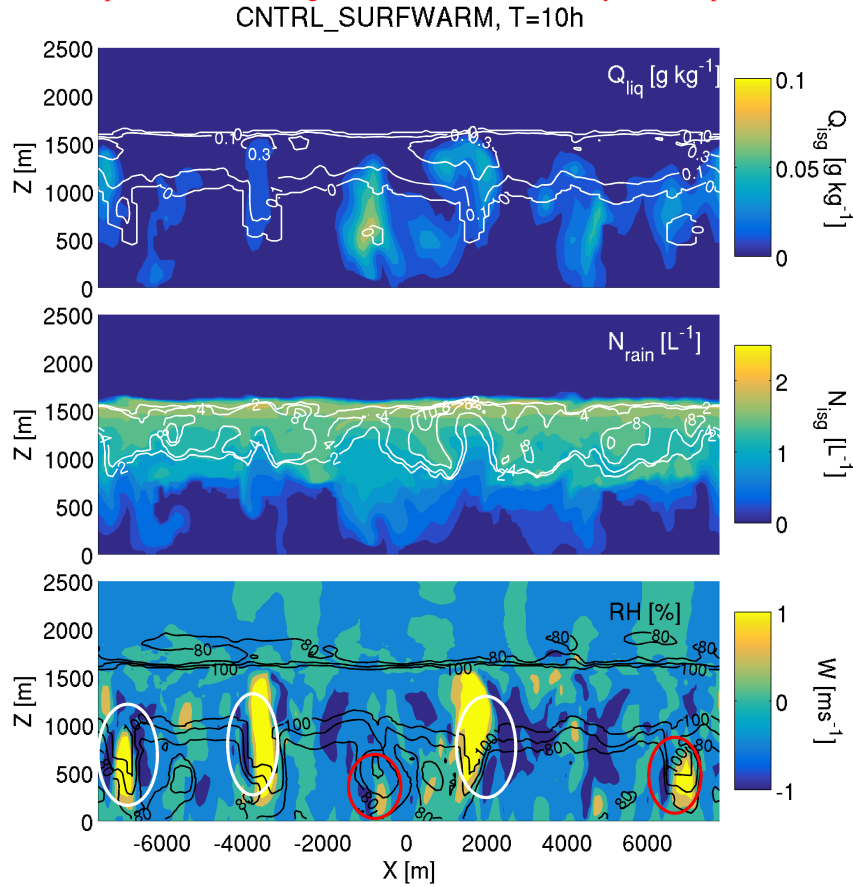


Figure 11. Z-X slices for the CNTRL_SURFWARM case at 10 h. **Top row:** total ice mass mixing ratio (Q_{isg} , shading) and liquid water mass mixing ratio (Q_{liq} , contours). **Middle row:** total ice number concentration (ice+snow+graupel, N_{isg} , shading) and rain number concentration (N_{rain} , contours). **Bottom row:** vertical velocity (W , shading) and relative humidity (RH, contours). Identified detached below-cloud cumuli are highlighted by red ellipses, and cumuli merged with the Sc are indicated by white ellipses.

The CNTRL_SURFWARM simulation experiences a sharp burst of TKE at cloud top 10 h, at which point the bottom-up propagation from the surface appears to fully couple the BL. Within approximately 1.5 h, the TKE sources decouple again. Z-X slices of several microphysical variables from CNTRL_SURFWARM are shown in Fig. 11 to sample illustrate the cloud structure at 10 h. In the bottom panel, below-cloud cumuli form which either couple to the Sc layer (white ellipses) or remain separate (red ellipses). These cumuli structures are clearly visible in the Q_{liq} contour field (top panel, Fig. 11). Cumuli are identified by adjacent updraught/downdraught regions with 100 % RH (or close to 100 %). These cumuli structures are clearly

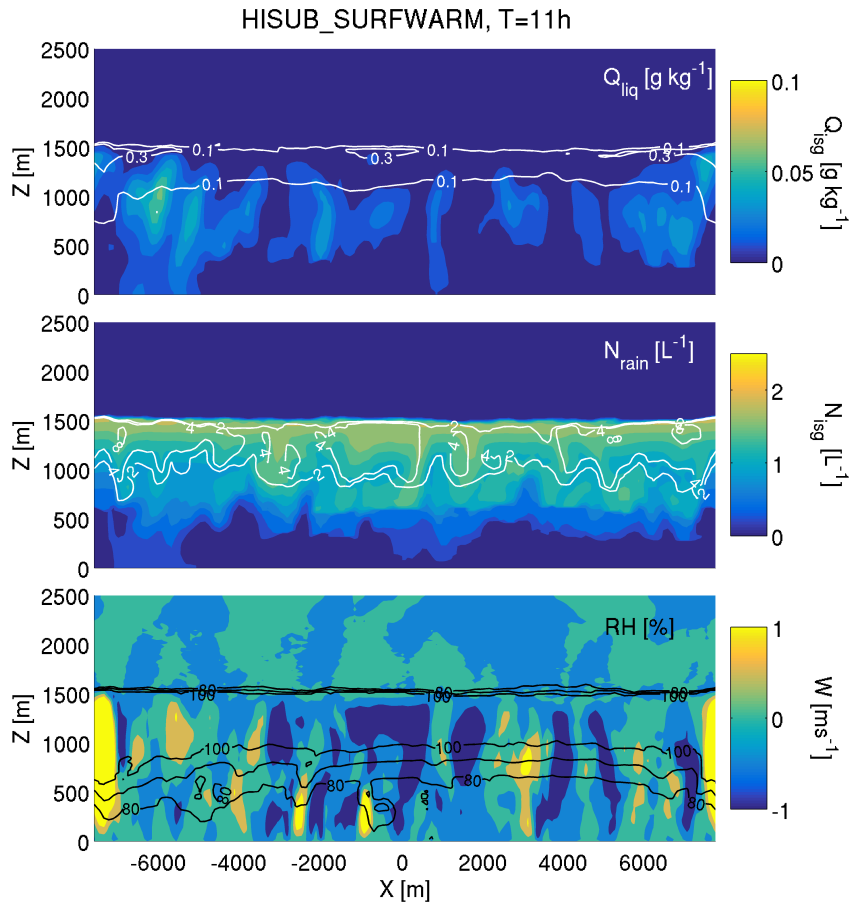


Figure 12. Z-X slices for the HISUB_SURFWARM case at 12 h. Panels are arranged similarly to Fig. 11.

visible in the Q_{liq} contour field (top panel, Fig. 11). Cumuli can be seen from 8 h onwards, and become more frequent with time. ~~Two~~ At this time, two spatially-close cumuli form at approximately -7000 m and -3500 m which mark, marking the boundaries of a detraining layer of moisture above cloud top. Additionally, a similar, completely detached moist layer can be seen above cloud top coinciding with the 6000 m cumulus.

- 5 ~~Total ice number concentrations (ice + snow + graupel, N_{isg} , Fig. 11b) are largely unaffected by the dynamical stimulation of the cloud by the warming surface whereas, as previously found when imposing subsidence (test 1, Sect. 3.1), the liquid phase (both Q_{liq} and N_{rain}) is positively influenced. In particular, N_{rain} in CNTRL_SURFWARM is much more comparable with the corresponding domain-averaged values of the LO- and HISUB_Ndrop50 simulations in test 2 (Fig. 5B) — the efficient liquid precipitation cases — than any of the previous control simulations.~~
- 10 ~~Similar to without surface forcing (Fig. S5), strong downdraughts form at lower altitudes in the Se-layer in HISUB_SURFWARM, likely forced by heightened evaporative cooling below cloud (Fig. 12). HISUB_SURFWARM has much larger updraught and downdraught regions than CNTRL_SURFWARM: from approximately 11 h onwards, these often extend to almost the full~~

height of the BL (Fig. 12). No distinct sub-cloud cumuli ~~are can be~~ identified in HISUB_SURFWARM (Fig. 12), whereas these are common in CNTRL_SURFWARM (Fig. 11): the addition of subsidence acts to suppress their formation and allow a more homogeneous Sc layer to be maintained in a BL undergoing top-down and bottom-up coupling of TKE. ~~In test 1, this coupling was primarily driven by the cloud TKE sources, whereas the extra input from the warming surface here leads to a more coupled TKE profile than without.~~ The coupling process is more gradual in HISUB_SURFWARM than the CNTRL or LOSUB counterparts, suggesting that subsidence plays a role in whether or not this rapid TKE coupling and cloud top ascent can take place.

4 Discussion

4.1 Effect of subsidence on bulk cloud properties

10 Imposing large-scale subsidence in simulations of marine ~~sub-Aretic-Arctic~~ mixed-phase Sc increases the LWP and IWP of the modelled clouds through increased convective activity throughout the domain (Fig. 2). W_{sub} does not affect the cloud ~~extent-depth~~ (Fig. 5, 7); only N_{ice} notably affects the modelled cloud depth (Fig. 6). Dynamical stimulation by subsidence – which would sustain a mixed-phase Sc for longer against the WBF mechanism – may therefore have been previously missed in observations and modelling studies. Increasing W_{sub} has a greater effect on the liquid phase than the ice phase (Figs. 2, 4, 6);
15 however, increasing subsidence causes the development of heterogeneity in the LWP and IWP fields, leading to instabilities in the modelled clouds. In particular, the radiative properties of the clouds would be affected by the heterogeneous spread in LWP, where regions of high LWP would be more reflective to incoming shortwave radiation (Schröter et al., 2005) and more efficiently cooled via longwave radiative cooling.

Localised regions of high IWP are typically co-located with updraughts in our simulations, likely due to the method of
20 parameterising ice nucleation in our model. Namely, additional nucleation mechanisms (e.g. contact, immersion) are not represented ~~such that we have to give us~~ a predictable source of ice number concentrations (similar to Young et al., 2017). These mechanisms would likely influence our results if they were explicitly resolved in our model; for example, we would expect contact nucleation in downdraughts, through interaction with interstitial aerosol particles.

Subsidence strongly influences the LWP; however, increasing ~~levels of subsidence also marginally increase~~ W_{sub} ~~marginally~~
25 ~~increases~~ the domain-averaged IWP (Fig. 2b). Figure 6(b) shows that the peak IWP attained by CNTRL_D10x2 is also achieved in the HISUB_D10 case, suggesting that increasing W_{sub} can have a similar effect on the bulk ice properties of the cloud as increasing N_{ice} . However, a much larger LWP is also modelled when subsidence is imposed, creating a microphysical structure that may be more robust against the WBF mechanism. This may allow mixed-phase conditions to be sustained for longer against a higher N_{ice} ; a problem that is often faced when modelling Arctic mixed-phase Sc (Harrington and Olsson, 2001;
30 Prenni et al., 2007; Morrison et al., 2012; de Boer et al., 2011, 2014; Young et al., 2017).

4.2 Effect of subsidence on microphysics and precipitation

In the chosen microphysical scenarios that may affect precipitation development in ~~marine~~ mixed-phase ~~Sc~~, ~~large-scale subsidence~~ ~~marine Sc~~, W_{sub} enhances rain evaporation at cloud top and base. Increased subsidence leads to larger rain ~~mass~~ production rates and a greater N_{rain} within cloud, and this effect is particularly clear when lowering ~~either~~ N_{drop} (Ndrop50, Fig. 5) or ~~lowering~~ N_{ice} (D10 \times 0.5, Fig. 7) ~~in tests 2 and 3 respectively~~. In these cases, the increase in N_{rain} due to subsidence is less than can be attributed to the ~~imposed~~ microphysical changes; for example, an increase of approximately 6 L^{-1} is modelled in the Ndrop50 scenario due to increasing W_{sub} , whilst an increase of approximately 9 L^{-1} is achieved by lowering N_{drop} from 100 cm^{-3} to 50 cm^{-3} (Fig. 5B).

From ~~test-tests 2~~, ~~we can conclude that large-scale subsidence and 3~~, W_{sub} amplifies the modelled turbulence in scenarios allowing for efficient ~~precipitation formation~~ (~~rain formation~~ (e.g. Ndrop50, Fig 4i). ~~In fact~~, W_{sub} also acts to promote ~~more~~ turbulence (Fig. 4k) and rain formation (Fig. 5B) in a microphysical scenario that produces little rain in its absence (Ndrop150). Conversely, increasing N_{ice} in test 3 does not have the same effect, and ~~increasing~~ W_{sub} does little to promote turbulence in this scenario. ~~Increased snow number concentrations and production/sublimation rates do not have the same dynamical effect on these clouds as similar changes in the rain category, and the combined cooling from rain evaporation at cloud base and radiative cooling at cloud top causes the efficient development of convection in these liquid-dominated clouds. These findings indicate that subsidence has the potential to positively force the liquid phase of these clouds whilst having little effect on the ice phase. Young et al. (2016) presented observations of cloud microphysics over the transition from sea ice to ocean and found that the ice phase changed little under the dynamical evolution of the BL, while the liquid water content increased four-fold. Our findings therefore suggest that mixed-phase clouds with low number concentrations of primary ice, such as those commonly observed in the springtime Arctic, are vulnerable to dynamical changes induced by subsiding air from above or a warming surface from below.~~

~~Increasing N_{ice} (test 3) produces more $N_{\text{s+g}}$ as expected, and this increase does not have the same dynamical effect as decreasing N_{drop} (and producing more rain). However, whilst~~ ~~Whilst~~ the ice categories do little to stimulate convection, they are responsible for suppressing rain formation; for example, a higher N_{ice} (and thus, $N_{\text{s+g}}$) suppresses the strong rain production/evaporation processes modelled at a lower N_{ice} (Fig. 7B). With weakened rain formation and evaporation (~~Fig. 7B~~), less vigorous overturning is modelled in D10 \times 2. ~~Increased snow number concentrations, and production and sublimation rates, do not have the same dynamical impact on these clouds as the production/evaporation of rain~~ ~~2 than D10 or D10 \times 0.5~~. Whilst the liquid phase drives the development of dynamical overturning, the ice phase has a strong influence – through the WBF mechanism – on whether this convective activity can actually develop.

~~All modelled rain does not reach the surface; in all of our simulations, strong rain evaporation occurs below cloud. These findings are in contrast to cloud-resolving model simulations of warm convective clouds by Feingold et al. (2015). Simulations shown in~~ ~~Similarly, total ice number concentrations (ice+snow+graupel, N_{isg} , Fig. 11b) are largely unaffected by a warming surface (with comparison to Fig. 2 display a similar heterogeneity in W and LWP as the warm non-drizzling Sc case modelled by Savijärvi and Stevens (2008). All rain produced by our simulations evaporates below cloud; therefore, they could be~~

termed "non-drizzling". However, it is important to note that precipitation as snow is modelled in every case shown, and this snow always reaches the surface. Observational studies of Arctic marine mixed-phase Sc (Young et al., 2016) and North Atlantic CAOs (Abel et al., 2017) have previously reported precipitation as snow below cloud with little to no rain measured, indicating that our idealised modelling study is in broad agreement with measurements in this region.

5 The LO- and HISUB_SURFWARM cases, like their test 1 counterparts, continue to produce heightened rain evaporation below cloud, introducing a negative $w'\Theta'$ flux to the middle of the BL (S3b); however, both Q_{liq} and N_{rain} increase. Precipitation formation is enhanced in downdraught regions (Figs. 11, 12). Weaker below-cloud rain evaporation occurs in CNTRL_SURFWARM (Fig. 10e), and the upward propagation of heat and moisture from the surface causes distinct cumuli to form below cloud and join with cloud base. These cumuli dynamically stimulate the cloud from below (Fig. 11) and have a similar effect on the cloud as the introduction of subsidence in tests 1–3; for example, the warming surface allows a greater N_{rain} to form in cloud (Fig. 11). In the absence of strong subsidence, namely in CNTRL and LOSUBfact, N_{rain} in CNTRL_SURFWARM, the warming surface acts to push cloud top higher, and increase the LWP, through the formation of these below-cloud cumuli. This may suggest that, in regions of low subsidence, cloud top height may be forced upwards by a warming surface, causing strong heterogeneities to form in the spatial distribution of the LWP (Fig. 9d), leaving the cloud layer vulnerable to the formation of strong convective cells with motion southwards.

15 is much more comparable with the corresponding domain-averaged values of the LO- and HISUB_Ndrop50 simulations in test 2 (Fig. 5B) – the efficient liquid precipitation cases – than any of the previous control simulations.

These findings indicate that subsidence has the potential to positively force the liquid phase in Arctic mixed-phase marine Sc whilst having little effect on the ice phase. Young et al. (2016) presented observations of cloud microphysics over the transition from sea ice to ocean and found that the ice phase changed little under the dynamical evolution of the BL, while the liquid water content increased four-fold. Therefore, mixed-phase clouds with low number concentrations of primary ice, such as those commonly observed in the springtime Arctic, may be vulnerable to dynamical changes induced by subsiding air from above or a warming surface from below.

4.3 Effect of subsidence on the BL and dynamics

25 Convective activity increases in the modelled clouds. In tests 1–3, convective activity increases with W_{sub} through increased BL TKE and below-cloud w'^2 ; in test 1–3. Solar heating acts to marginally offset the formation of defined closed-cellular structure; however, the cloud-driven convection is strongly dependent on cloud top LW radiative cooling (see Supplement, Fig. S6). Additionally, rain mass formation rates, number concentrations, and the domain-averaged LWP increase with increasing W_{sub} . This finding mirrors the conclusions of Hill et al. (2014), where the authors found that increasing the resolved TKE and/or temperature positively influences the liquid phase in ice saturated conditions an ice saturated environment, as these conditions contribute towards sustaining water saturation.

30 With a larger LWP, stronger cloud top radiative cooling is expected, promoting a greater cloud top height (Wang and Feingold, 2009a). Subsidence acts to restrict cloud top ascent by reinforcing the BL temperature inversion (Table 2), thus lowering the entrainment rate of air from above. Cloud LWP increases in the absence of notable dry-air entrainment, allowing for stronger cloud top

LW radiative cooling and subsequent precipitation development within cloud. As a result, BL temperatures are cooler with imposed subsidence than without (Fig. 3i), due to the combined effect of reduced entrainment, strong cloud top radiative cooling and enhanced evaporative cooling below cloud. Additionally, the sub-cloud layer becomes more moist and well-mixed with increasing levels of subsidence (Fig. 3a–c) as below-cloud rain evaporation generates TKE and promotes convective overturning in the BL. These findings are consistent with observations of precipitating pockets of open cells (POCs), where rain evaporation below cloud was found to cool and moisten the BL (vanZanten and Stevens, 2005).

surface warming, all modelled BLs display a stable Θ_{il} profile. This stability is likely influenced by the stable conditions used to initialise the model, and one must note that only a single set of initial conditions were used in this study. A moist layer is maintained close to the surface in the CNTRL simulation (Fig. 3a), below the sub-cloud mixed layer, whereas this moisture source is eroded in the subsidence cases. Additionally, the CNTRL case presents a minor BL Θ_{il} inversion, and a stronger Q_{tot} inversion, at approximately 500 m. The combination of these inversions and the moist surface layer suggests that the CNTRL simulation is, in fact, more strongly decoupled from the surface than the subsidence cases at the time step shown (9 h, Fig. 3). However, the subsidence cases display a similar strongly decoupled profile in TKE as the CNTRL at earlier times (e.g. 5 h, Fig. 3). TKE increases with time in the BL when subsidence is imposed, and appears to promote top-down mixing of TKE through the sub-cloud layer towards the surface by the end of the simulations, tending towards a coupled profile. With more convection caused by strong rain evaporation below cloud, more BL mixing occurs. However, cloud top TKE still dominates the BL profiles in the LO- and HISUB cases (Fig. 3b, c), suggesting that mixing throughout the BL is still not homogeneous and the clouds remain approximately decoupled from the surface by the termination time of the simulations. This decoupling allows radiative cooling at cloud top and evaporative cooling/latent heating below cloud to drive convective activity in the cloud layers, irrespective of surface sources.

With a larger LWP, stronger cloud top radiative cooling is expected, promoting a greater cloud top height (Wang and Feingold, 2009a). Subsidence acts to restrict cloud top ascent by reinforcing the BL temperature inversion (Table 2), thus lowering the entrainment rate of air from above. Cloud LWP increases in the absence of notable entrainment, allowing for stronger cloud top LW radiative cooling and subsequent precipitation development within cloud. BL temperatures are therefore cooler with imposed subsidence than without (Fig. 3i), due to the combined effect of reduced entrainment, strong cloud top radiative cooling, and enhanced evaporative cooling below cloud.

When consistent surface temperatures and large-scale subsidence are modelled, W_{sub} acts to promote convection through heightened TKE at cloud top and strong evaporation below cloud. This effect appears to be linearly-related to the magnitude of W_{sub} . The opposite effect occurs when a combination of subsidence and a lack of subsidence combined with a warming surface is imposed: higher levels of subsidence acts to push cloud top significantly higher, and increase the LWP, through the formation of the below-cloud cumuli (namely in CNTRL and LOSUB_SURFWARM, Fig. 9d). Higher levels of W_{sub} act to stabilise the Sc layer and suppress the formation of cumuli from the warming surface (as is seen in the CNTRL_SURFWARM case). TKE production is positively influenced in the CNTRL and LOSUB_SURFWARM cases, with strongly separated cloud and surface sources, and peak values approximately three times greater than modelled in test 1 (Tables 2 and 3). $w^2\Theta'$ and w^2Q_{vap}' are significantly larger below cloud in CNTRL_SURFWARM at the time step shown in

Fig. 10(h,i) due to the formation of the below-cloud cumuli; these do not form in HISUB_SURFWARM, and far fewer form in LOSUB_SURFWARM. Cloud top TKE splits in two in both CNTRL and LOSUB_SURFWARM (Fig. 10a,b); however, it is unlikely that this is a resolution domain artefact as the vertical resolution is consistent through this altitude range. It is possible that the PW advection scheme is introducing spurious oscillations into the advected quantities, caused by the sharp gradient at the cloud boundary (as discussed by Gray et al., 2001), due to the formation of these dynamic cumuli (as discussed by Gray et al., 2001). Peak TKE is only marginally stronger in HISUB_SURFWARM than in test 1 (Tables 2 and 3), suggesting that the higher level subsidence offsets higher W_{sub} offsets the efficient in-cloud TKE production which occurs when the system is additionally forced by a warming surface.

The gradual coupling of TKE sources seen in HISUB_SURFWARM is likely influenced by the strong evaporative cooling below cloud, which acts to offset the two sources of strong heat and moisture fluxes and make the coupling process more stable. By suppressing the formation of below-cloud cumuli, subsidence acts to produce a stable, yet dynamic, Sc layer, whilst strong convection and spatial heterogeneity are simulated with low or no subsidence. With more heterogeneity, there is an increased likelihood for instability in the cloud layer, which will likely influence the fate of the cloud downstream.

4.4 Role of domain resolution

Whilst CAOs are discussed to motivate our study, we must stress that our chosen domain configuration is not optimal for the explicit study of Sc-to-cumulus transitions downstream in a CAO. Large, high resolution domains are required to accurately resolve the small-scale microphysical processes within these phenomena (Field et al., 2014); however, our domain size and resolution are restricted by computational expense. Bretherton et al. (1999) demonstrated that our spatial resolution may allow entrainment rates to be overpredicted by approximately 50% (Connolly et al., 2013). Whilst the authors concluded that the resolutions resolution imposed here can still provide a useful insight into BL evolution, accurately-resolved turbulence requires a higher model higher spatial resolution. Feingold et al. (2015) found that a higher-resolution setup produces produced enhanced BL convection and a deeper BL depth. By increasing spatial resolution Furthermore, Wang and Feingold (2009a) found that the simulated vertical mixing of vapour and Θ fields improved, and the modelled LWP increased, in their open cellular convection simulations by increasing spatial resolution.

To test the influence of resolution on our findings, we increase the horizontal resolution to 60 m (Δx) and the vertical resolution to 10 m, whilst maintaining the domain height. This setup therefore decreases the spatial extent of the domain by half in both X and Y. Vertical resolution was 10 m up to 2000 m, decreasing to 20 m above this height. By increasing our model resolution, we aim to provide a more accurate representation of the modelled entrainment rates. Due to computational expense, only two test cases are considered; the CNTRL and HISUB simulations from test 1 (Sec. 3.1).

~~Influence of domain resolution on changing imposed large-scale subsidence. Only the CNTRL and HISUB cases are considered. LWP (a) and IWP (b) time series for simulations with 120 m resolution (default configuration) and 60 m resolution (high resolution configuration). **Black:** CNTRL, default, **grey:** CNTRL, high resolution, **red:** HISUB, default, and **pink:** HISUB, high resolution. **c-h:** Vertical profiles (at 9 h) of (c): solid precipitation (snow + graupel) tendency, (d): rain tendency ($\partial N_{rain}/\partial t$), (e): ice-liquid potential temperature (Θ_{ll} , solid) and total water mixing ratio (Q_{tot} , dashed), (f): buoyancy flux~~

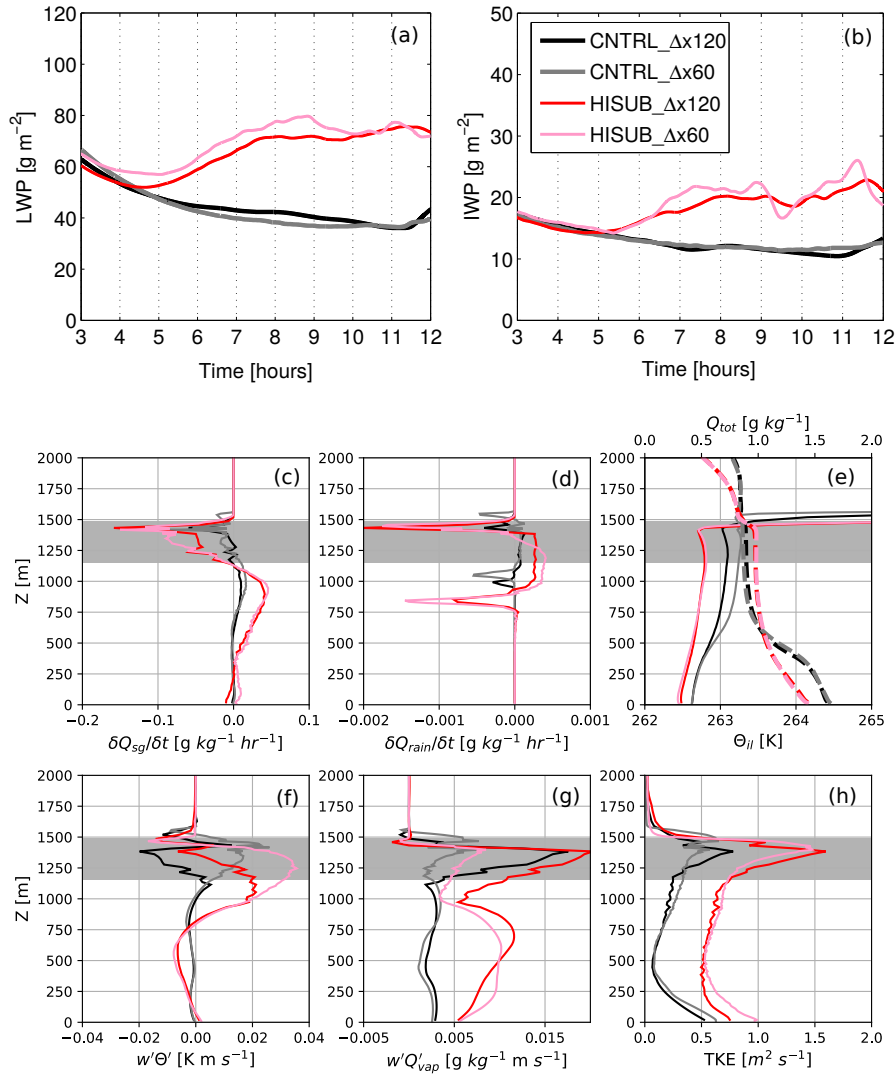


Figure 13. Influence of domain resolution on changing imposed large-scale subsidence. Only the CNTRL and HISUB cases are considered. LWP (a) and IWP (b) time series for simulations with 120 m resolution (default configuration) and 60 m resolution (high resolution configuration). **Black:** CNTRL, default, **grey:** CNTRL, high resolution, **red:** HISUB, default, and **pink:** HISUB, high resolution. **c–h:** Vertical profiles (at 9 h) of (c): solid precipitation (snow + graupel) mass tendency ($\delta Q_{sg}/\delta t$), (d): rain mass tendency ($\delta Q_{rain}/\delta t$), (e): ice-liquid potential temperature (Θ_{il} , solid) and total water mixing ratio (Q_{tot} , dashed), (f): buoyancy flux ($w'\Theta'$), (g): vertical flux of water vapour ($w'Q_{vap}'$) and (h): total turbulent kinetic energy (TKE). Fluxes shown are total quantities (sub-grid + advected). Area in grey represents CNTRL_Δx120m cloudy regions.

($w'\Theta'$), (g): vertical flux of water vapour ($w'Q_{vap}'$) and (h): total turbulent kinetic energy (TKE). Fluxes shown are total quantities (sub-grid + advected). Area in grey represents CNTRL $\Delta x 120m$ cloudy regions.

The influence of increasing model resolution on the LWP and IWP in the CNTRL setup is shown by the black and the grey traces in Figs. 13(a,b). Little difference between the domain-averaged LWP and IWP can be identified between these CNTRL cases the CNTRL cases (black/grey, Figs. 13a,b). In the HISUB example—where the higher resolution is shown in pink and the default in red—, increasing the model resolution amplifies the irregularities in both the LWP and IWP traces. In particular, the IWP is significantly more variable with time than in the CNTRL setup. Adding a high level of large-scale subsidence and increasing the model resolution allows for more vigorous convective activity to develop with comparison to our CNTRL simulations.

10 In general, increasing the resolution does not alter the trends identified previously; for example, the positive below-cloud moisture fluxes, higher below-cloud rain evaporation mass evaporation and snow mass growth rates, and increased TKE with increasing W_{sub} . In fact, it should be noted that the below cloud rain below cloud rain mass evaporation rates are enhanced with comparison to the coarse resolution HISUB case, suggesting that the evaporation rates shown in Sects. 3.2, 3.3, and 3.4 may be underestimated. Increased rain evaporation rates at cloud top may be influencing the snow sublimation rates: with more rain evaporating, the humidity may be maintained above the ice supersaturation threshold, thus suppressing the rate at which snow sublimates. Increasing the vertical resolution allows a greater peak N_{rain} to be modelled, whilst little difference can be identified with N_{s+g} (not shown, Fig. ??); therefore, there is more rain available to evaporate, sustaining the humidity above ice supersaturation. The Q_{tot} profiles illustrate clear decoupling in the CNTRLs, with a weaker inversion in the HISUB cases. Additionally, both $\Delta x 60$ simulations produce a greater TKE peak towards the surface, in addition to the peak simulated at cloud top, due to the dominating influence of the sub-grid contribution to the TKE towards the surface.

(Fig. 13b).

Whilst we can test the influence of increased resolution on our findings, increasing our domain size would be too computationally expensive for our setup. Larger domains are often used to allow mesoscale interactions between developing open convective cells to be resolved. Schröter et al. (2005) suggest that a domain of 100×100 km, with 50–100 m spatial resolution, is required to truly encapsulate any mesoscale interactions between developing convective cells in CAOs. We cannot speculate what mesoscale interactions may occur between the different scenarios presented here; however, one must note that such interactions have been previously simulated to occur over the transition between closed and open convective cells in CAOs, thus these effects should be investigated in further work.

4.5 Broader implications

30 Increased convection is modelled within mixed-phase BL Sc with increased subsidence, driven by radiative cooling at cloud top and rain evaporative cooling at cloud base. By enforcing the BL temperature inversion, subsidence reduces entrainment rates from above and thus allows for a greater LWP (and often, IWP) and efficient precipitation development. With more precipitation evaporating below cloud—coupled with efficient LW radiative cooling at cloud top—the cloud layers become more convective, with increased TKE throughout the BL. These dynamic clouds will be better sustained against the WBF

mechanism. This is a crucial result for the understanding of mixed-phase Sc in the Arctic — particularly in the Arctic spring — where high pressure, stable conditions dominate across the region. These clouds have been observed to persist for long periods of time, and subsidence caused by large-scale meteorology could be acting to sustain these clouds microphysically against dissipation or glaciation. Kay and Gettelman (2009) found lower cloud fractions in high pressure regions; however, it is important to note that this study considered the high Arctic, where the surface was ice-covered. Our results indicate a microphysical sensitivity to subsiding air associated with high pressure systems in the ocean-exposed low-, or sub-, Arctic regions; regions which commonly experience CAOs.

5 Conclusions

Large-scale subsidence is often imposed in LES models as a tuning factor to maintain cloud top height; however, the influence of this parameter on mixed-phase cloud microphysics has not been previously investigated. Here, we have shown how large-scale subsidence affects the microphysical structure of BL Arctic mixed-phase marine Sc using the UK Met Office Large Eddy Model (LEM, UK Met Office, Gray et al., 2001). By subjecting four idealised scenarios – a stable Sc, varied droplet (N_{drop}) or ice (N_{ice}) number concentrations, and a warming surface – to different levels of subsidence, we have identified a clear relationship between subsidence and convection development, with potential implications for mixed-phase BL clouds forming in the ocean-exposed low-, or sub-, Arctic regions.

Key features identified in this study are as follows:

- With no surface forcing (tests 1–3), increasing the imposed large-scale subsidence (W_{sub}) reinforces the BL temperature inversion and thus reduces entrainment from the free troposphere. With less dry air from aloft mixing into the clouds, a greater LWP (and often, IWP) develops, allowing for efficient precipitation development, cloud top radiative cooling, and downdraught production. Precipitation formation is enhanced in these downdraught regions, and all All of the rain produced evaporates below cloud. The combination of strong cloud top radiative and cooling, below-cloud evaporative cooling, rain evaporative cooling, and latent heating from snow growth at cloud base generates more TKE within the BL, leading to enhanced turbulent overturning throughout the cloud layer, positively forcing the LWP. These linked processes. These three requirements combine to form a feedback loop consisting of W_{sub} , LWP, rain evaporation LWP, below-cloud rain evaporation/snow growth, and TKE development.
- Imposed large-scale subsidence has a greater impact on the LWP and IWP than the chosen microphysical changes; varying N_{drop} (Fig. 4) or N_{ice} (Fig. 6). BL TKE, w'^2 , and cloud LWP increase with increasing, positively forced by the magnitude of W_{sub} , suggesting that the clouds may be more robust against dissipation or glaciation via the WBF mechanism. Quiescent, less dynamic clouds are modelled under no subsidence; clouds which may be more vulnerable to the WBF mechanism.
- In microphysical scenarios which promote efficient rain production (low N_{drop} or low N_{ice}), W_{sub} enhances rain mass production and evaporation rates, TKE at cloud top and at the surface, and turbulent activity throughout the BL. Modelled

N_{rain} increases with W_{sub} , whilst ~~snow number concentrations marginally decrease~~ N_{sg} ~~marginally decreases~~. Modelled rain evaporates ~~more efficiently than snow, and stimulates efficiently, coinciding with regions of snow growth. These microphysical processes stimulate~~ the cloud dynamically by introducing perturbations in moisture and temperature below cloud. Only precipitation as snow reaches the surface, mirroring observations of ~~marine~~ mixed-phase ~~marine~~ Sc in the Arctic (~~Young et al., 2016~~) and in CAOs.

- ~~– Subsidence affects both the liquid and ice phases when properties related to the liquid phase are altered (test 2, Fig. 4). However, altering Altering the ice phase feeds back onto the liquid phase through the influence of the WBF mechanism (test 3, Fig. 6). Clouds with greater ice number concentrations suppress the liquid phase; therefore, N_{ice} has a key role in mediating the strength of turbulent overturning induced in these mixed-phase clouds . Subsidence readily affects the concentration of rain produced through convective overturning, whilst the ice phase is relatively insensitive to these changes by suppressing the liquid phase. However, N_{ice} is also a crucial component at the opposite end of the scale: there needs to be enough ice present to produce enough latent heating via depositional growth to force convection from cloud base. With more dynamical motion ~~in the modelled cloud~~, the liquid phase may be sustained more effectively against the WBF mechanism.~~
- ~~– In the absence of surface warming, all modelled BLs display a stable Θ_{T} profile; however, cloud sources of TKE, moisture, and heat are decoupled from the surface due to strong below-cloud rain evaporation. This decoupling allows radiative cooling at cloud top and evaporative cooling below cloud to drive convective activity in the cloud layers, irrespective of surface sources. The HISUB simulation tends towards a coupled, well-mixed BL through the top-down and bottom-up propagation of TKE (test 1, Fig. 3c) This is a crucial result for the understanding of mixed-phase Sc in the Arctic – particularly in the Arctic spring – where high pressure, stable conditions are common across the region. These clouds have been observed to persist for long periods of time, and subsidence caused by large-scale meteorology could be acting to sustain these clouds microphysically against dissipation or glaciation.~~
- ~~– The feedbacks identified from test 1–3 are not so clearly related when a warming surface is additionally imposed: significantly larger values of $w'Q_{\text{vap}}$ ' and $w'\Theta'$ are modelled with no W_{sub} , coinciding with the rapid BL coupling shown in Fig. 10(a). In-cloud rain production rates produced in CNTRL_SURFWARM are also much greater than ~~modelled~~ without surface forcing in test 1. A warming surface, and a lack of subsidence, acts to dynamically stimulate the modelled cloud from below, similar to how subsidence stimulates it from above.~~
- ~~– Below-cloud cumuli form in CNTRL_SURFWARM, and to a lesser extent in LOSUB_SURFWARM, which act to push cloud top higher, generate high LWP, and cause significant spatial heterogeneity in the cloud layer. This cumuli formation is suppressed when under high levels of subsidence (HISUB_SURFWARM); the combination of these two forcings counteract one another to produce a stable, yet dynamic, Sc layer.~~
- ~~– In all subsidence cases, the Θ_{T} profiles become unstable towards the warm surface. The CNTRL_SURFWARM case couples strongly at 10 h (Fig. 10a,b), whilst the dominating cloud sources of TKE in HISUB_SURFWARM allows the~~

~~cloud to couple more gradually to surface TKE, moisture, and heat sources. The gradual coupling of HISUB_SURFWARM is likely influenced by the strong evaporative cooling below cloud (test 6, Fig. 10e).~~

- ~~– Similar to our coarse resolution simulations, more in-cloud and surface TKE is modelled in HISUB_Δx60 than in CNTRL_Δx60. Increasing model resolution exaggerates the effect of imposing large-scale subsidence. Below-cloud rain evaporation rates and in-cloud $w'\theta'$ increase with increasing resolution, whilst $BL \Theta_{11}$ and TKE are largely unaffected.~~

This study presents a clear relationship between large-scale subsidence and the development of convection in liquid-dominated mixed-phase clouds common to the ~~sub-Arctic~~ Arctic. We propose that the influence of large-scale subsidence in both ~~sub-Arctic CAOs and~~ Arctic mixed-phase Sea-marine Sc and CAOs should be considered in further work, ~~with using~~ with using models of different spatial scales. In particular, it would be beneficial to study the development of CAO flows – with a high-resolution, large domain – under a transitional profile of subsidence; i.e. flowing from a high pressure region. Our results suggest that a high W_{sub} will amplify turbulent activity and rain production/evaporation in any stable mixed-phase Sc modelled, and a weakening of subsidence alongside a warming surface will likely promote cloud top ascent, below-cloud cumuli formation, and strong spatial heterogeneities throughout the cloud layer. Therefore, further investigating the role of subsidence in CAO flows will be beneficial to our ability to accurately model and understand the break up of these cloud decks. More generally, comprehending the physical impact of subsidence on marine mixed-phase cloud microphysics at higher latitudes will allow us to better predict how clouds in the Arctic region may change in the depleted sea ice future.

6 Code availability

Please contact the UK Met Office for LEM code requests.

7 Data availability

LEM model runs are archived at the University of Manchester and are available on request.

Competing interests. The authors declare that they have no conflict of interest.

Acknowledgements. GY was funded by the National Environment Research Council (NERC) as part of the ACCACIA campaign (grant NE/I028696/1). PJC acknowledges funding from EU FP7 project BACCHUS (grant agreement no. 603445).

References

- Abel, S. J., Boutle, I. A., Waite, K., Fox, S., Brown, P. R. A., Cotton, R., Lloyd, G., Choullarton, T. W., and Bower, K. N.: The role of precipitation in controlling the transition from stratocumulus to cumulus clouds in a northern hemisphere cold-air outbreak, *J. Atmos. Sci.*, doi:10.1175/JAS-D-16-0362.1, in press, 2017.
- 5 Bodas-Salcedo, A., Williams, K. D., Field, P. R., and Lock, A. P.: The Surface Downwelling Solar Radiation Surplus over the Southern Ocean in the Met Office Model: The Role of Midlatitude Cyclone Clouds, *Journal of Climate*, 25, 7467–7486, doi:10.1175/JCLI-D-11-00702.1, 2012.
- Bretherton, C. S., Macvean, M. K., Bechtold, P., Chlond, A., Cotton, W. R., Cuxart, J., Cuijpers, H., Mhairoutdinov, M., Kosovic, B., Lewellen, D., Moeng, C.-H., Siebesma, P., Stevens, B., Stevens, D. E., Sykes, I., and Wyant, M. C.: An intercomparison of radiatively
10 driven entrainment and turbulence in a smoke cloud, as simulated by different numerical models, *Quarterly Journal of the Royal Meteorological Society*, 125, 391–423, doi:10.1002/qj.49712555402, 1999.
- Bryan, G. H. and Fritsch, J. M.: A Reevaluation of Ice–Liquid Water Potential Temperature, *Monthly Weather Review*, 132, 2421–2431, doi:10.1175/1520-0493(2004)132<2421:AROIWP>2.0.CO;2, 2004.
- Connolly, P. J., Vaughan, G., Cook, P., Allen, G., Coe, H., Choullarton, T. W., Dearden, C., and Hill, A.: Modelling the effects of gravity
15 waves on stratocumulus clouds observed during VOCALS-UK, *Atmospheric Chemistry and Physics*, 13, 7133–7152, doi:10.5194/acp-13-7133-2013, 2013.
- Curry, J. A., Ebert, E. E., and Herman, G. F.: Mean and turbulence structure of the summertime Arctic cloudy boundary layer, *Quarterly Journal of the Royal Meteorological Society*, 114, 715–746, doi:10.1002/qj.49711448109, 1988.
- de Boer, G., Morrison, H., Shupe, M. D., and Hildner, R.: Evidence of liquid dependent ice nucleation in high-latitude stratiform clouds from
20 surface remote sensors, *Geophysics Research Letters*, 38, L01803, doi:10.1029/2010GL046016, 2011.
- de Boer, G., Shupe, M. D., Caldwell, P. M., Bauer, S. E., Persson, O., Boyle, J. S., Kelley, M., Klein, S. A., and Tjernström, M.: Near-surface meteorology during the Arctic Summer Cloud Ocean Study (ASCOS): evaluation of reanalyses and global climate models, *Atmospheric Chemistry and Physics*, 14, 427–445, doi:10.5194/acp-14-427-2014, 2014.
- de Boer, G., Shupe, M. D., Caldwell, P. M., Bauer, S. E., Persson, O., Boyle, J. S., Kelley, M., Klein, S. A., and Tjernström, M.: Near-surface
25 meteorology during the Arctic Summer Cloud Ocean Study (ASCOS): evaluation of reanalyses and global climate models, *Atmospheric Chemistry and Physics*, 14, 427–445, doi:10.5194/acp-14-427-2014, 2014.
- Dee, D. P., Uppala, S. M., Simmons, A. J., Berrisford, P., Poli, P., Kobayashi, S., Andrae, U., Balmaseda, M. A., Balsamo, G., Bauer, P., Bechtold, P., Beljaars, A. C. M., van de Berg, L., Bidlot, J., Bormann, N., Delsol, C., Dragani, R., Fuentes, M., Geer, A. J., Haimberger, L., Healy, S. B., Hersbach, H., Hólm, E. V., Isaksen, I., Kållberg, P., Köhler, M., Matricardi, M., McNally, A. P., Monge-Sanz, B. M., Morcrette, J.-J., Park, B.-K., Peubey, C., de Rosnay, P., Tavolato, C., Thépaut, J.-N., and Vitart, F.: The ERA-Interim reanalysis:
30 configuration and performance of the data assimilation system, *Quarterly Journal of the Royal Meteorological Society*, 137, 553–597, doi:10.1002/qj.828, 2011.
- DeMott, P. J., Prenni, A. J., Liu, X., Kreidenweis, S. M., Petters, M. D., Twohy, C. H., Richardson, M. S., Eidhammer, T., and Rogers, D. C.: Predicting global atmospheric ice nuclei distributions and their impacts on climate, *Proceedings of the National Academy of Sciences*,
35 doi:10.1073/pnas.0910818107, 2010.
- Feingold, G., Koren, I., Wang, H., Xue, H., and Brewer, W. A.: Precipitation-generated oscillations in open cellular cloud fields, *Nature*, 466, 849–852, doi:10.1038/nature09314, 2010.

- Feingold, G., Koren, I., Yamaguchi, T., and Kazil, J.: On the reversibility of transitions between closed and open cellular convection, *Atmospheric Chemistry and Physics*, 15, 7351–7367, doi:10.5194/acp-15-7351-2015, 2015.
- Field, P. R., Cotton, R. J., McBeath, K., Lock, A. P., Webster, S., and Allan, R. P.: Improving a convection-permitting model simulation of a cold air outbreak, *Quarterly Journal of the Royal Meteorological Society*, 140, 124–138, doi:10.1002/qj.2116, 2014.
- 5 Fletcher, J., Mason, S., and Jakob, C.: The Climatology, Meteorology, and Boundary Layer Structure of Marine Cold Air Outbreaks in Both Hemispheres, *Journal of Climate*, 29, 1999–2014, doi:10.1175/JCLI-D-15-0268.1, 2016.
- Gray, M. E. B., Petch, J. C., Derbyshire, S. H., Brown, A. R., Lock, A. P., Swann, H. A., and Brown, P. R. A.: Version 2.3 of the Met Office Large Eddy Model: Part II. Scientific Documentation., Tech. rep., 2001.
- Harrington, J. Y. and Olsson, P. Q.: On the potential influence of ice nuclei on surface-forced marine stratocumulus cloud dynamics, *Journal of Geophysical Research: Atmospheres*, 106, 27 473–27 484, doi:10.1029/2000JD000236, 2001.
- 10 Harrington, J. Y., Reisin, T., Cotton, W. R., and Kreidenweis, S. M.: Cloud resolving simulations of Arctic stratus. Part II: Transition-season clouds, *Atmospheric Research*, 51, 45–75, doi:10.1016/S0169-8095(98)00098-2, 1999.
- Hill, A. A., Field, P. R., Furtado, K., Korolev, A., and Shipway, B. J.: Mixed-phase clouds in a turbulent environment. Part 1: Large-eddy simulation experiments, *Quarterly Journal of the Royal Meteorological Society*, 140, 855–869, doi:10.1002/qj.2177, 2014.
- 15 Karlsson, J. and Svensson, G.: The simulation of Arctic clouds and their influence on the winter surface temperature in present-day climate in the CMIP3 multi-model dataset, *Climate Dynamics*, 36, 623–635, doi:10.1007/s00382-010-0758-6, 2011.
- Kay, J. E. and Gettelman, A.: Cloud influence on and response to seasonal Arctic sea ice loss, *Journal of Geophysical Research (Atmospheres)*, 114, D18204, doi:10.1029/2009JD011773, 2009.
- Kazil, J., Feingold, G., Wang, H., and Yamaguchi, T.: On the interaction between marine boundary layer cellular cloudiness and surface heat 20 fluxes, *Atmospheric Chemistry and Physics*, 14, 61–79, doi:10.5194/acp-14-61-2014, 2014.
- Kolstad, E. W., Bracegirdle, T. J., and Seierstad, I. A.: Marine cold-air outbreaks in the North Atlantic: temporal distribution and associations with large-scale atmospheric circulation, *Climate Dynamics*, 33, 187–197, doi:10.1007/s00382-008-0431-5, 2009.
- Leonard, B. P., MacVean, M. K., and Lock, A. P.: Positivity- preserving numerical schemes for multidimensional advection, *NASA Technical Memorandum*, 1993.
- 25 Morrison, H., Curry, J. A., and Khvorostyanov, V. I.: A New Double-Moment Microphysics Parameterization for Application in Cloud and Climate Models. Part I: Description, *Journal of Atmospheric Sciences*, 62, 1665–1677, doi:10.1175/JAS3446.1, 2005.
- Morrison, H., de Boer, G., Feingold, G., Harrington, J., Shupe, M. D., and Sulia, K.: Resilience of persistent Arctic mixed-phase clouds, *Nature Geoscience*, 5, 11–17, doi:10.1038/ngeo1332, 2012.
- Müller, G. and Chlond, A.: Three-dimensional numerical study of cell broadening during cold-air outbreaks, *Boundary-Layer Meteorology*, 30 81, 289–323, doi:10.1007/BF02430333, 1996.
- Myers, T. A. and Norris, J. R.: Observational Evidence That Enhanced Subsidence Reduces Subtropical Marine Boundary Layer Cloudiness, *Journal of Climate*, 26, 7507–7524, doi:10.1175/JCLI-D-12-00736.1, 2013.
- Ovchinnikov, M., Korolev, A., and Fan, J.: Effects of ice number concentration on dynamics of a shallow mixed-phase stratiform cloud, *Journal of Geophysical Research (Atmospheres)*, 116, D00T06, doi:10.1029/2011JD015888, 2011.
- 35 Ovchinnikov, M., Ackerman, A. S., Avramov, A., Cheng, A., Fan, J., Fridlind, A. M., Ghan, S., Harrington, J., Hoose, C., Korolev, A., McFarquhar, G. M., Morrison, H., Paukert, M., Savre, J., Shipway, B. J., Shupe, M. D., Solomon, A., and Sulia, K.: Intercomparison of large-eddy simulations of Arctic mixed-phase clouds: Importance of ice size distribution assumptions, *Journal of Advances in Modeling Earth Systems*, 6, 223–248, doi:10.1002/2013MS000282, 2014.

- Piacsek, S. and Williams, G.: Conservation Properties of Convection Difference Schemes, *J Comp Phys*, 6, 393–405, 1970.
- Prenni, A. J., Harrington, J. Y., Tjernström, M., DeMott, P. J., Avramov, A., Long, C. N., Kreidenweis, S. M., Olsson, P. Q., and Verlinde, J.: Can Ice-Nucleating Aerosols Affect Arctic Seasonal Climate?, *Bulletin of the American Meteorological Society*, 88, 541–550, doi:10.1175/BAMS-88-4-541, 2007.
- 5 Rosenfeld, D., Wang, H., and Rasch, P. J.: The roles of cloud drop effective radius and LWP in determining rain properties in marine stratocumulus, *Geophysical Research Letters*, 39, doi:10.1029/2012GL052028, 113801, 2012.
- Sandu, I. and Stevens, B.: On the Factors Modulating the Stratocumulus to Cumulus Transitions, *Journal of the Atmospheric Sciences*, 68, 1865–1881, doi:10.1175/2011JAS3614.1, 2011.
- Savic-Jovcic, V. and Stevens, B.: The Structure and Mesoscale Organization of Precipitating Stratocumulus, *Journal of the Atmospheric*
 10 *Sciences*, 65, 1587–1605, doi:10.1175/2007JAS2456.1, 2008.
- Schröter, M., Raasch, S., and Jansen, H.: Cell Broadening Revisited: Results from High-Resolution Large-Eddy Simulations of Cold Air Outbreaks, *Journal of the Atmospheric Sciences*, 62, 2023–2032, doi:10.1175/JAS3451.1, 2005.
- Shipway, B. J. and Hill, A. A.: Diagnosis of systematic differences between multiple parametrizations of warm rain microphysics using a kinematic framework, *Quarterly Journal of the Royal Meteorological Society*, 138, 2196–2211, doi:10.1002/qj.1913, 2012.
- 15 Solomon, A., Shupe, M. D., Persson, P. O. G., and Morrison, H.: Moisture and dynamical interactions maintaining decoupled Arctic mixed-phase stratocumulus in the presence of a humidity inversion, *Atmospheric Chemistry and Physics*, 11, 10 127–10 148, doi:10.5194/acp-11-10127-2011, 2011.
- Solomon, A., Feingold, G., and Shupe, M. D.: The role of ice nuclei recycling in the maintenance of cloud ice in Arctic mixed-phase stratocumulus, *Atmospheric Chemistry and Physics*, 15, 10 631–10 643, doi:10.5194/acp-15-10631-2015, 2015.
- 20 Stramler, K., Genio, A. D. D., and Rossow, W. B.: Synoptically Driven Arctic Winter States, *Journal of Climate*, 24, 1747–1762, doi:10.1175/2010JCLI3817.1, 2011.
- Trenberth, K. E. and Fasullo, J. T.: Simulation of Present-Day and Twenty-First-Century Energy Budgets of the Southern Oceans, *Journal of Climate*, 23, 440–454, doi:10.1175/2009JCLI3152.1, 2010.
- Tripoli, G. J. and Cotton, W. R.: The Use of Ice-Liquid Water Potential Temperature as a Thermodynamic Variable In Deep Atmospheric
 25 *Models*, *Monthly Weather Review*, 109, 1094–1102, doi:10.1175/1520-0493(1981)109<1094:TUOLLW>2.0.CO;2, 1981.
- van der Dussen, J. J., de Roode, S. R., and Siebesma, A. P.: How large-scale subsidence affects stratocumulus transitions, *Atmospheric Chemistry and Physics*, 16, 691–701, doi:10.5194/acp-16-691-2016, 2016.
- vanZanten, M. C. and Stevens, B.: Observations of the Structure of Heavily Precipitating Marine Stratocumulus, *Journal of the Atmospheric Sciences*, 62, 4327–4342, doi:10.1175/JAS3611.1, 2005.
- 30 Walsh, J. E., Phillips, A. S., Portis, D. H., and Chapman, W. L.: Extreme Cold Outbreaks in the United States and Europe, 1948–99., *Journal of Climate*, 14, 2642–2658, doi:10.1175/1520-0442(2001)014<2642:ECOITU>2.0.CO;2, 2001.
- Wang, H. and Feingold, G.: Modeling Mesoscale Cellular Structures and Drizzle in Marine Stratocumulus. Part I: Impact of Drizzle on the Formation and Evolution of Open Cells, *Journal of the Atmospheric Sciences*, 66, 3237–3256, doi:10.1175/2009JAS3022.1, 2009a.
- Wang, H. and Feingold, G.: Modeling Mesoscale Cellular Structures and Drizzle in Marine Stratocumulus. Part II: The Microphysics
 35 and Dynamics of the Boundary Region between Open and Closed Cells, *Journal of the Atmospheric Sciences*, 66, 3257–3275, doi:10.1175/2009JAS3120.1, 2009b.
- Wang, H., Feingold, G., Wood, R., and Kazil, J.: Modelling microphysical and meteorological controls on precipitation and cloud cellular structures in Southeast Pacific stratocumulus, *Atmospheric Chemistry and Physics*, 10, 6347–6362, doi:10.5194/acp-10-6347-2010, 2010.

- Wood, R., Bretherton, C. S., Leon, D., Clarke, A. D., Zuidema, P., Allen, G., and Coe, H.: An aircraft case study of the spatial transition from closed to open mesoscale cellular convection over the Southeast Pacific, *Atmospheric Chemistry and Physics*, 11, 2341–2370, doi:10.5194/acp-11-2341-2011, 2011.
- Yamaguchi, T. and Feingold, G.: On the relationship between open cellular convective cloud patterns and the spatial distribution of precipitation, *Atmospheric Chemistry and Physics*, 15, 1237–1251, doi:10.5194/acp-15-1237-2015, 2015.
- 5 Young, G., Jones, H. M., Choulaton, T. W., Crosier, J., Bower, K. N., Gallagher, M. W., Davies, R. S., Renfrew, I. A., Elvidge, A. D., Darbyshire, E., Marengo, F., Brown, P. R. A., Ricketts, H. M. A., Connolly, P. J., Lloyd, G., Williams, P. I., Allan, J. D., Taylor, J. W., Liu, D., and Flynn, M. J.: Observed microphysical changes in Arctic mixed-phase clouds when transitioning from sea ice to open ocean, *Atmospheric Chemistry and Physics*, 16, 13 945–13 967, doi:10.5194/acp-16-13945-2016, 2016.
- 10 Young, G., Connolly, P. J., Jones, H. M., and Choulaton, T. W.: Microphysical sensitivity of coupled springtime Arctic stratocumulus to modelled primary ice over the ice pack, marginal ice, and ocean, *Atmospheric Chemistry and Physics*, 17, 4209–4227, doi:10.5194/acp-17-4209-2017, 2017.

Supplementary Material

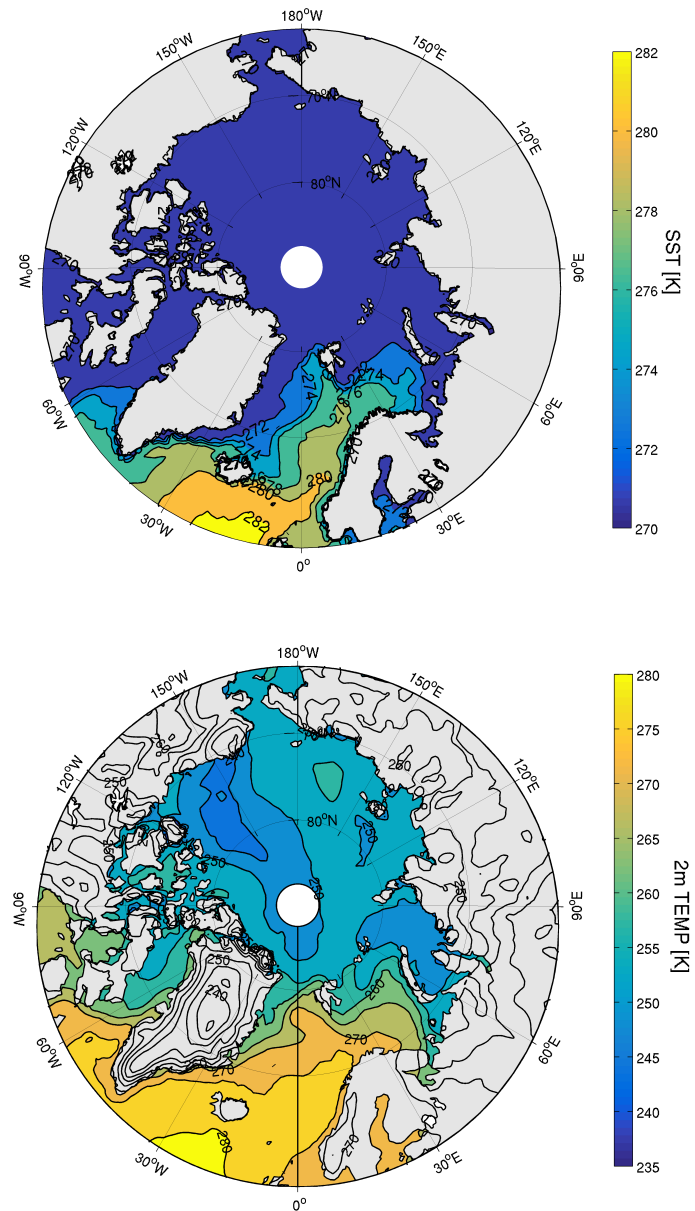


Figure S1. ERA-Interim (ECMWF Reanalysis, Dee et al., 2011) data for sea surface temperature (SST, top panel) and 2 m temperature (bottom panel) on 23 March 2013. These data were used as a guide to construct a surface warming profile. Data used to initialise the LEM – from Young et al. (2017) – were simulated on this day.

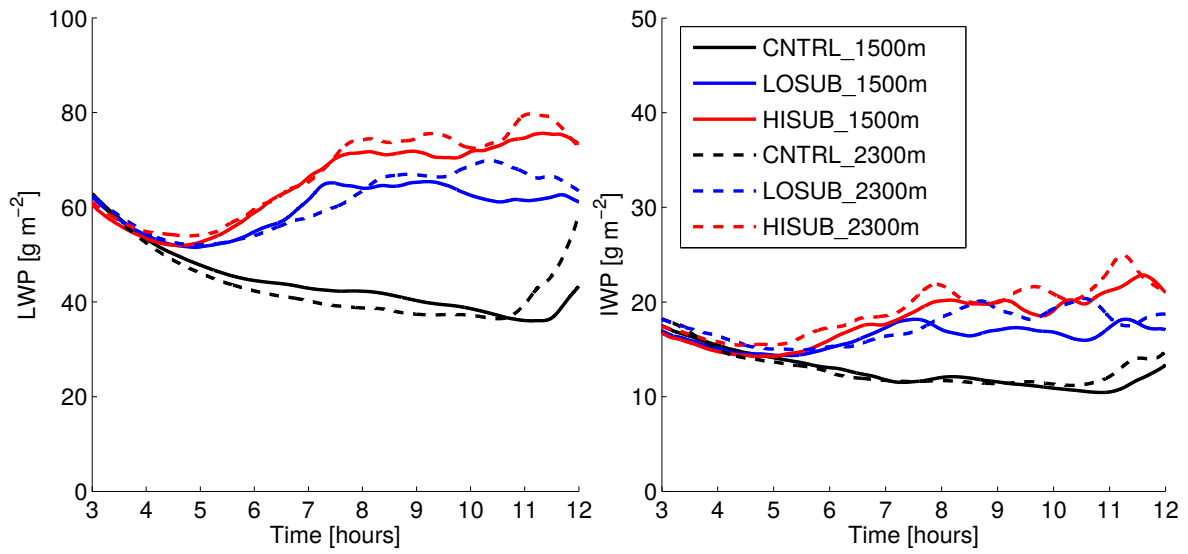


Figure S2. Domain-averaged liquid- and ice-water path time series for the runs detailed in test 1 (solid lines) and those with more Z levels added (dashed lines). Runs listed with the suffix `_2300m` have more vertical levels added: 20 m resolution is imposed up to 2300 m, above which it decreases to 50 m. The trends identified in Sect. 3.1 (greater LWP/IWP with imposed subsidence) are largely unaffected by the addition of more high resolution levels across the BL inversion.

Rain particle number concentration (N_{rain} , left panel) and snow+graupel number concentration ($N_{\text{s+g}}$, right panel) modelled at 9 h in the simulations listed in the legend. Peak N_{rain} increases in the HISUB cases with increased vertical resolution, whilst this quantity decreases under a similar change in the CNTRL cases. $N_{\text{s+g}}$ is not strongly affected by the increase in resolution.

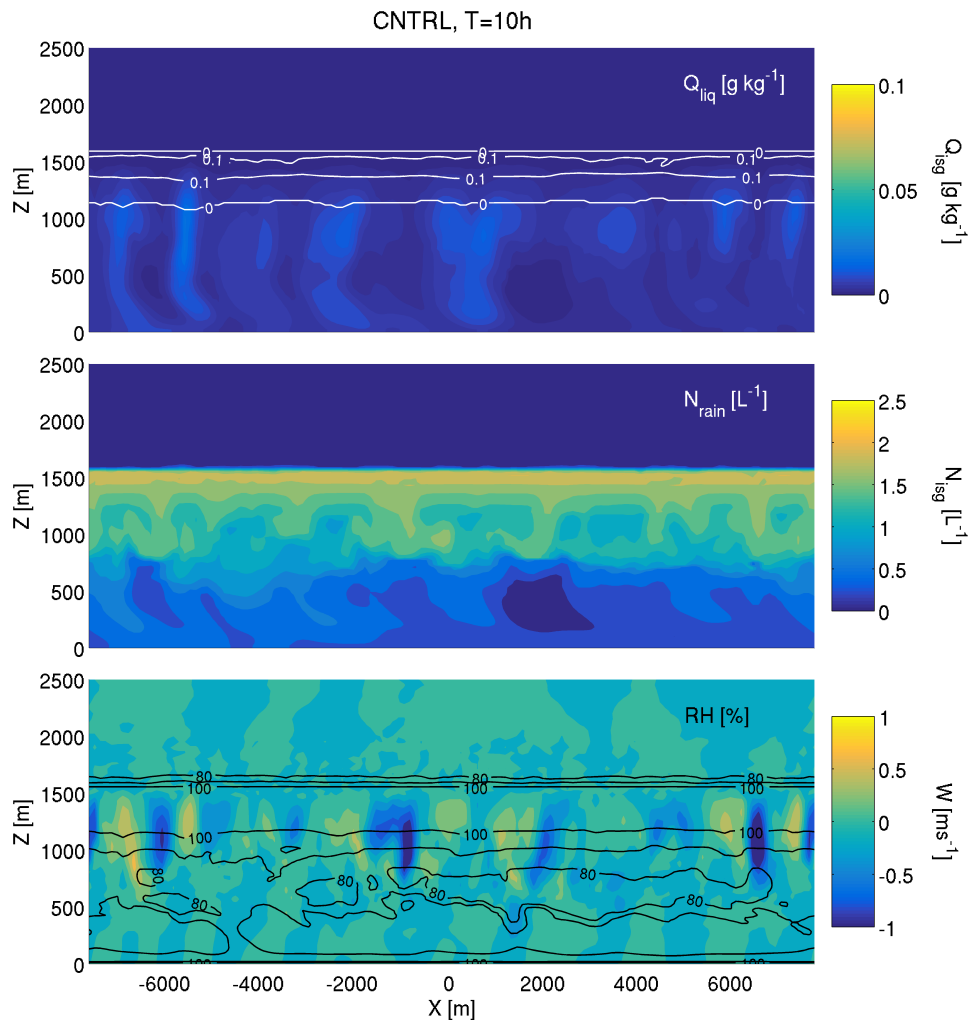


Figure S3. Z-X slices for the CNTRL case at 10 h. **Top row:** total ice mass mixing ratio (Q_{iceg} , shading) and liquid water mass mixing ratio (Q_{liq} , contours). **Middle row:** total ice number concentration (N_{iceg} , shading) and rain number concentration (N_{rain} , contours). **Bottom row:** vertical velocity (W , shading) and relative humidity (RH, contours).

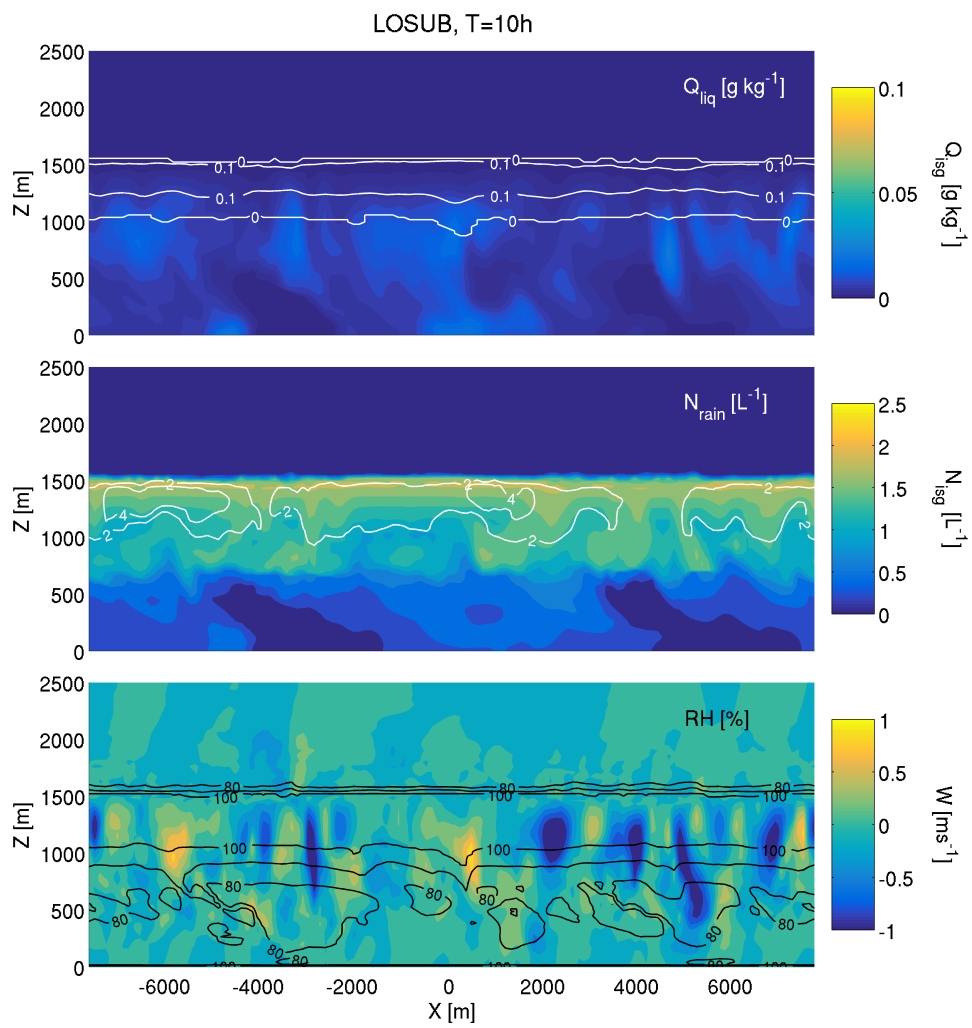


Figure S4. Z-X slices for the LOSUB case at 10 h, mirroring the format of Fig. S3.

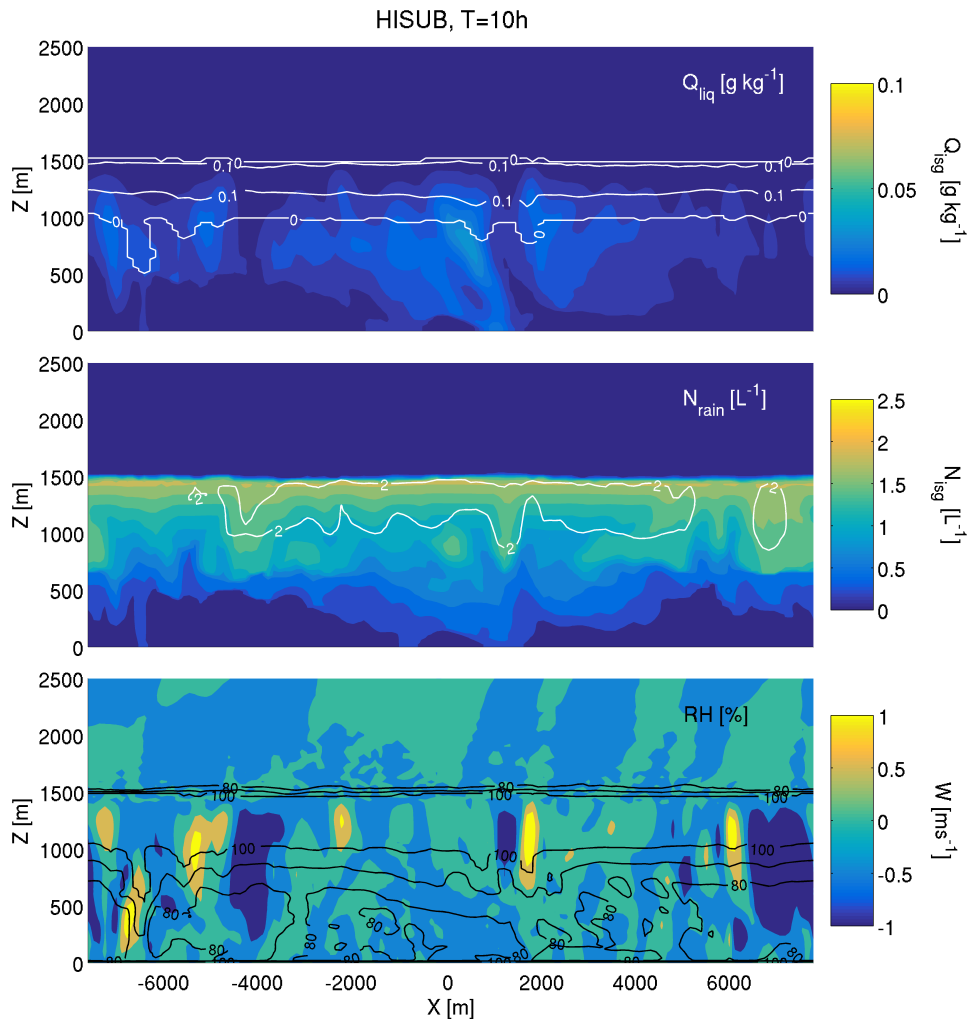


Figure S5. Z-X slices for the HISUB case at 10 h, mirroring the format of Fig. S3. In panel (c), strong updrafts and downdrafts are evident, with particularly broad downdraft regions. Pools of heightened RH occur at the bottom of these downdraft regions, co-located with elongated regions of N_{rain} in the Sc layer above.

Z-X slices for the LOSUB case at 10 h, mirroring the format of Fig. S3.

Z-X slices for the HISUB case at 10 h, mirroring the format of Fig. S3.

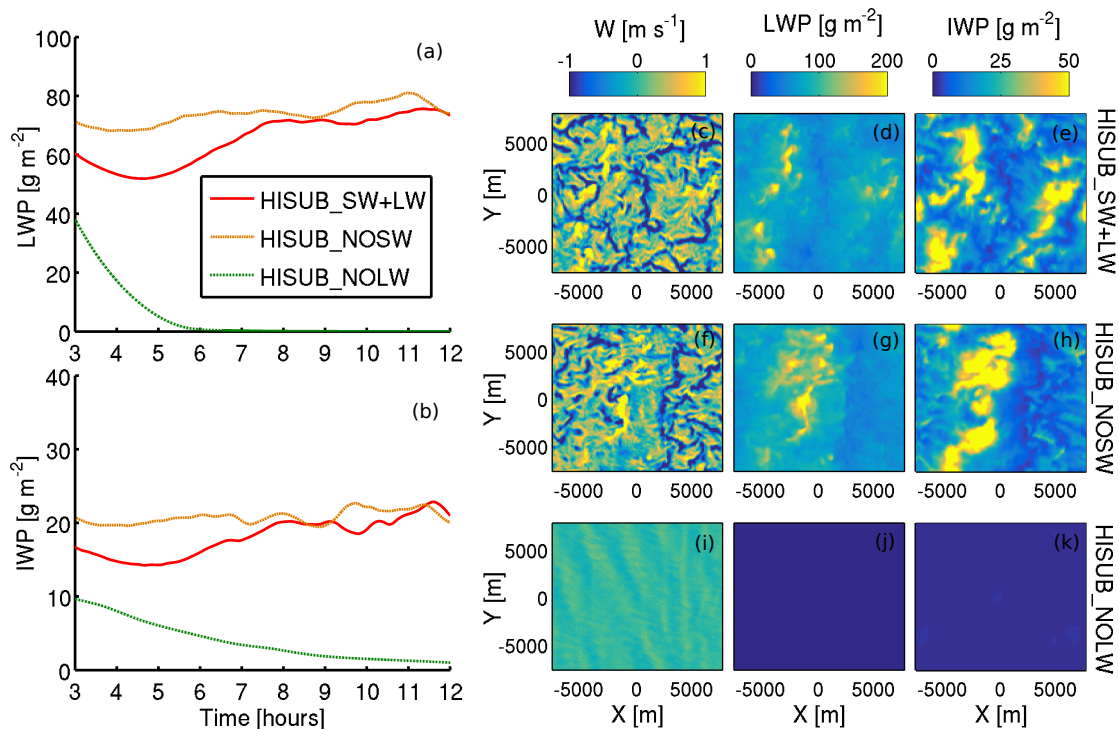


Figure S6. Relationship between subsidence-induced convection and radiation. **(a, b):** Time series of the domain-averaged LWP and IWP from HISUB simulations with both shortwave (SW) and longwave (LW) switched on (red), only LW on (orange), and only SW on (green). **(c–k):** Planar X-Y views of **(c,f,i)** vertical velocity, W , at 1000 m, **(d,g,j)** LWP, and **(e,h,k)** IWP. Planar views shown at 11 h. Cloud lifetime is strongly dependent on longwave radiative cooling being represented in the model; ~~it dissipates~~ dissipation occurs quickly in its absence. Likewise, cloud heating by shortwave (solar) radiation is important to allow the development of the closed-cellular structure shown in panel c. Longwave radiative cooling at cloud top plays an important role in development of convection in the subsidence cases shown.

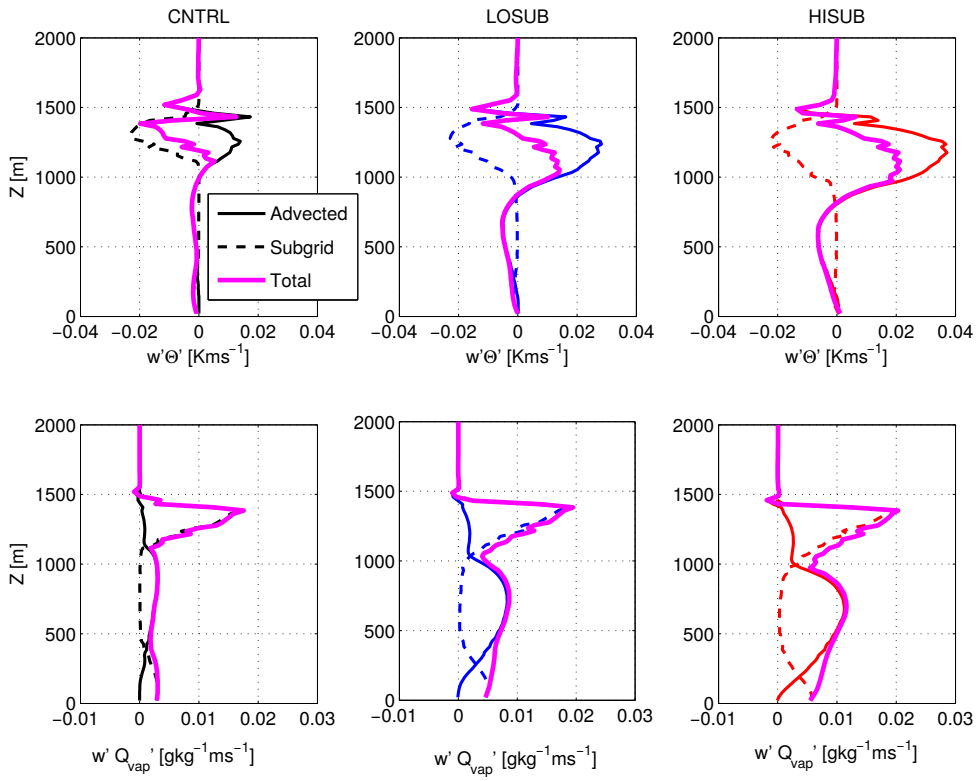


Figure S7. Relative contribution of advected (solid) and sub-grid (dashed) fluxes to the total (solid, magenta), $w'\Theta'$ (top row), and $w'Q_{vap}'$ at 9 h in test 1.

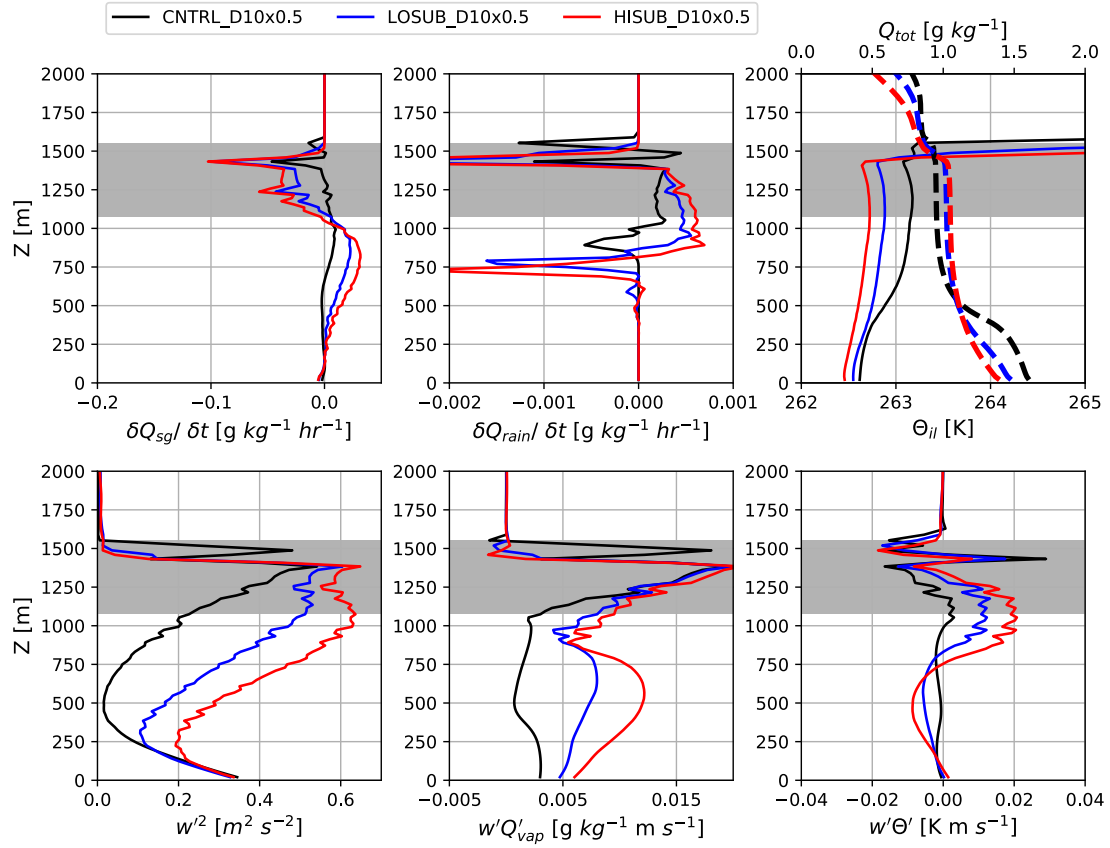


Figure S8. Vertical profiles, at 9 h, of solid precipitation (snow + graupel) mass tendency, rain mass tendency ($\delta Q_{rain}/\delta t$), ice-liquid potential temperature (Θ_{il} , solid) and total water mixing ratio (Q_{tot} , dashed), vertical velocity variance (w'^2), vertical flux of water vapour ($w'Q'_{vap}$) and buoyancy flux ($w'\Theta'$). w'^2 , $w'Q'_{vap}$, and $w'\Theta'$ are total quantities (sub-grid + advected). Area in grey represents LOSUBCNTRL_D10-D10x0.5 cloudy regions.

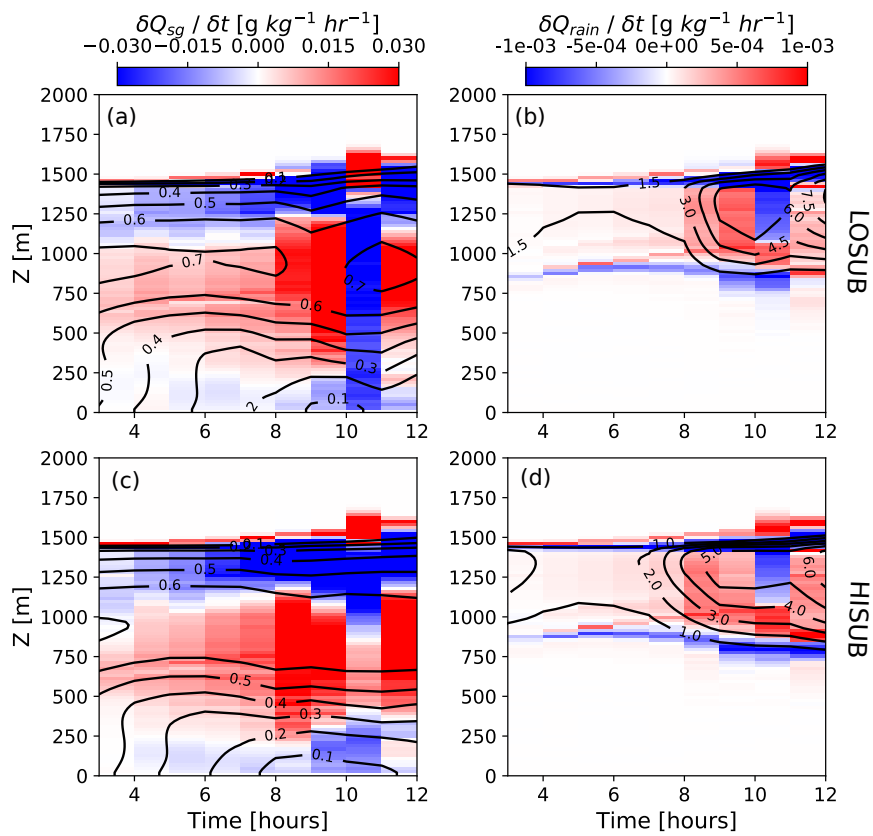


Figure S9. Arranged ~~similar~~ similarly to Fig. 5, showing the comparison between simulations with a warming surface (test 4).

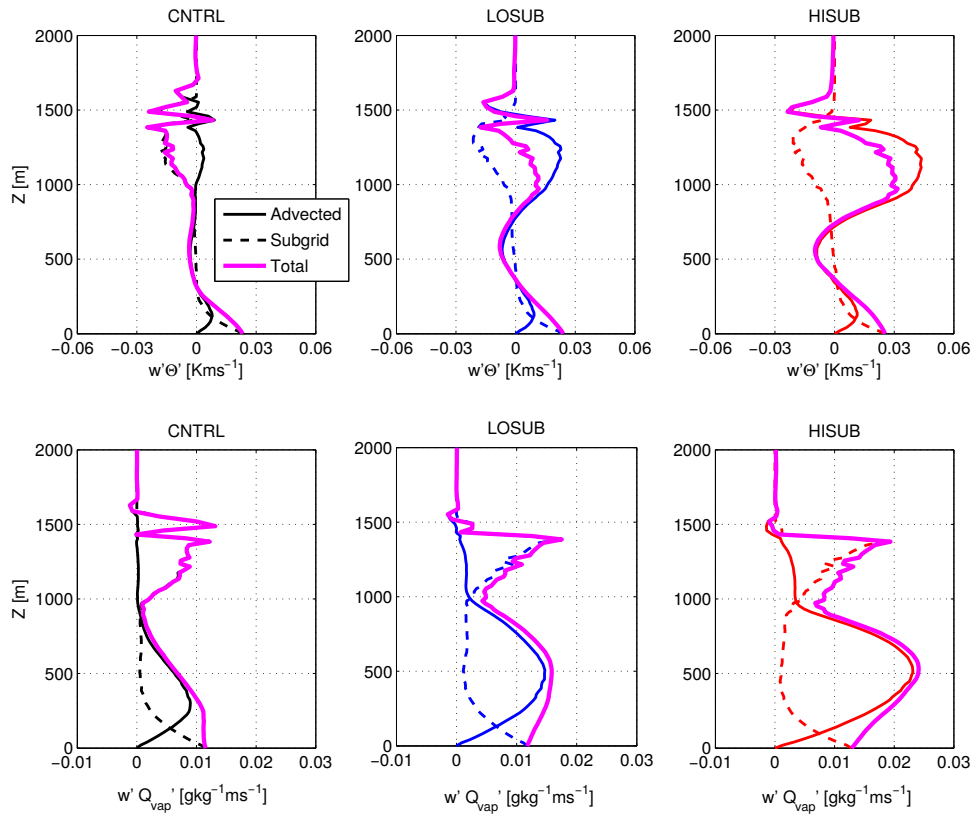


Figure S10. Relative contribution of advected (solid) and sub-grid (dashed) fluxes to the total (solid, magenta), $w'\Theta'$ (top row), and $w'Q_{vap}'$ at 11 h in test 6 (with surface forcing).